

The Proximal ID Algorithm

Ilya Shpitser

*Department of Computer Science
Johns Hopkins University
Baltimore, MD 21218, USA*

ILYAS@CS.JHU.EDU

Zach Wood-Doughty

*Department of Computer Science
Johns Hopkins University
Baltimore, MD 21218, USA*

ZACH@CS.JHU.EDU

Eric J. Tchetgen Tchetgen

*Department of Statistics
The Wharton School
3620 Locust Walk, Philadelphia, PA 19104, USA*

ETT@WHARTON.UPENN.EDU

Editor: Anonymous

Abstract

Unobserved confounding is a fundamental obstacle to establishing valid causal conclusions from observational data. Two complementary types of approaches have been developed to address this obstacle. An extensive line of work (Wright, 1928; Angrist and Krueger, 2001; Kuroki and Pearl, 2014) is based on taking advantage of fortuitous external aids (such as the presence of an instrumental variable or other proxy), along with additional assumptions to ensure identification. A recent line of work of *proximal causal inference* (Miao et al., 2018a; Tchetgen Tchetgen et al., 2020) has aimed to provide a novel approach to using proxies to deal with unobserved confounding without relying on stringent parametric assumptions.

On the other hand, a complete characterization of identifiability of a large class of causal parameters in arbitrary causal models with hidden variables has been developed using the language of graphical models, resulting in the ID algorithm and related extensions (Tian and Pearl, 2002; Shpitser and Pearl, 2006a,b; Huang and Valtorta, 2006; Shpitser and Sherman, 2018). Celebrated special cases of this approach, such as the front-door model (Pearl, 1995), are able to obtain non-parametric identification in seemingly counter-intuitive situations when a treatment and an outcome share an arbitrarily complicated unobserved common cause.

In this paper we aim to develop a synthesis of the proximal and graphical approaches to identification in causal inference to yield the most general identification algorithm in multivariate systems currently known – the proximal ID algorithm. In addition to being able to obtain non-parametric identification in all cases where the ID algorithm succeeds, our approach allows us to systematically exploit proxies to adjust for the presence of unobserved confounders that would have otherwise prevented identification.

In addition, we outline a class of estimation strategies for causal parameters identified by our method in an important special case. We illustrate our approach by simulation studies.

Keywords: causal inference; graphical models; identification; proximal causal inference

1. Introduction

Understanding cause effect relationships is a crucial task in empirical science and rational decision making. An extensive line of work spanning multiple communities has placed modern causal inference on a rigorous footing, using the language of potential outcomes, random variables representing responses to hypothetical interventions, as well as the language of graphical models and structural equations (Pearl, 2009; Richardson and Robins, 2013).

Modern causal inference conceptualizes cause effect relationships between treatments and outcomes using hypothetical randomized experiments implemented via an intervention operation (Pearl, 2009). Linking realizations of the observed data distribution with the counterfactual parameters arising in such experiments entails using assumptions encoded in causal models, with the resulting functionals estimated by plug-in estimators or semi-parametric methods (Van der Laan et al., 2003; Tsiatis, 2006).

As an example, if the causal relationship between a treatment variable A and an outcome Y is masked by spurious associations due to a vector of common causes \vec{C} , and all these causes are observed, then the average causal effect is identified by the covariate adjustment functional and estimated by matching methods, plug-in estimators, or the augmented inverse probability weighted estimator (Hernán and Robins, 2010; Robins et al., 1994).

If some of the relevant confounders are unobserved, the situation becomes considerably more difficult. In general, unobserved confounding prevents identification of causal parameters. However, a rich literature has been developed that exploits various kinds of causal and semi-parametric assumptions that allow point identification to be recovered. A complete characterization of identifiability of a large class of causal parameters in arbitrary causal models with hidden variables has been developed using the language of graphical models, resulting in the ID algorithm and related extensions (Tian and Pearl, 2002; Shpitser and Pearl, 2006a,b; Huang and Valtorta, 2006; Shpitser and Sherman, 2018). Celebrated special cases of this approach, such as the front-door model, are able to obtain non-parametric identification in seemingly counter-intuitive situations, such as when a treatment and an outcome share an arbitrarily complicated unobserved common cause.

An extensive complementary line of work on point identification in the presence of unobserved confounding (Wright, 1928; Angrist and Krueger, 2001; Kuroki and Pearl, 2014) is based on taking advantage of fortuitous external aids (such as the presence of an instrumental variable or other proxy), along with additional assumptions to ensure identification. A recent line of work of *proximal causal inference* (Miao et al., 2018a; Tchetgen Tchetgen et al., 2020) has aimed to provide a novel approach to using proxies to deal with unobserved confounding without relying on stringent parametric assumptions.

In this paper, we aim to unify these approaches by providing an approach to identification of counterfactual parameters in the presence of unobserved confounding, called the *proximal ID algorithm* that inherits the advantages of proximal inference and non-parametric identification via graphical models. Like the latter approach, the proximal ID algorithm is able to obtain point identification in multivariate structured systems with arbitrarily complex patterns of unobserved confounding, greatly extending the sets of cases where proximal inference may be used. At the same time, the proximal ID algorithm is able to exploit the presence of fortuitous proxies to obtain identification in cases where the ID algorithm would otherwise fail.

Our paper is organized as follows. In Section 2, we review the standard setting of proximal causal inference, largely following (Miao et al., 2018a; Tchetgen Tchetgen et al., 2020). In Section 3 we describe a nontrivial extension of this approach to settings where point identification may be obtained, despite the fact that the standard assumptions that proximal causal inference relies on fail. In Section 4, we describe the general theory of

non-parametric identification in graphical models and the ID algorithm as a prelude to the description of our main contribution, the proximal ID algorithm, in Section 5. In Section 6 we describe an important special case of the proximal ID algorithm, which applies proximal causal inference techniques to generalize the g-computation algorithm (Robins, 1986). Section 7 shows how identification theory developed in this paper may be used for identification of responses to treatment variables being counterfactually set according to a policy. Section 8 describes how existing statistical inference methods developed in the proximal causal inference literature (Miao et al., 2018b; Tchetgen Tchetgen et al., 2020) generalize to the example described in Section 3, and illustrates these methods via simulations. Section 9 contains our conclusions.

2. Notation and Illustration of Proximal Causal Inference

A standard setting in causal inference assumes the observed data realizations are i.i.d. samples from a distribution on a set of variables \vec{C}, A, Y , where A is a treatment or exposure of interest, Y is an outcome of interest, and \vec{C} are a set of baseline covariates. Cause effect relationships are conceptualized by means of potential outcome random variables. As an example, $Y(a)$ denotes the outcome Y had, possibly contrary to fact, treatment A was administered at value a . Potential outcomes are used to define counterfactual parameters, such as the population average causal effect: $\beta \equiv \mathbb{E}[Y(a)] - \mathbb{E}[Y(a')]$, where a represents the active treatment value, and a' the placebo or control treatment value. The goal of causal inference is to identify causal parameters such as β from the observed data distribution, such as $p(\vec{C}, A, Y)$, using causal assumptions that link counterfactual and observed data, and estimate the resulting identifying functional as efficiently and reliably as possible.

A standard assumption in causal inference states that observed outcomes equal counterfactual outcomes had treatments been set to their observed values. This assumption is known as *consistency* and is often written concisely as $Y = Y(A)$. Aside from consistency, additional assumptions are needed to point-identify counterfactual parameters. A popular causal model that yields identification of the population average causal effect is the conditionally ignorable or “backdoor” model. This model makes two crucial assumptions. The first is that treatment assignment and potential outcomes are independent given baseline covariates, that is $(Y(a) \perp\!\!\!\perp A \mid \vec{C})$, and the second is that all treatment values have support conditional on \vec{C} : $p(A = a \mid \vec{C}) > 0$ for all possible values a . Given these assumptions, as well as consistency, β is identified from $p(\vec{C}, A, Y)$ by the adjustment functional: $\mathbb{E}[\mathbb{E}[Y|a, \vec{C}] - \mathbb{E}[Y|a', \vec{C}]]$, which is a special case of the *g-formula* (Robins, 1986).

Algebraic restrictions in causal models, such as conditional ignorability, are often displayed visually by means of causal diagrams, particularly directed acyclic graphs (DAGs). The DAG representing the conditionally ignorable model is shown in Fig. 1 (a). This model implies that $\vec{C} \perp\!\!\!\perp A(\vec{c}_1) \perp\!\!\!\perp Y(a, \vec{c}_2)$ for any values $a \in \mathfrak{X}_A, \vec{c}_1, \vec{c}_2 \in \mathfrak{X}_{\vec{C}}$, and this in turn implies $(Y(a, \vec{C}) \perp\!\!\!\perp A(\vec{C}) \mid \vec{C})$ which is equivalent to $Y(a) \perp\!\!\!\perp A \mid \vec{C}$. This model may correspond to an observational study in healthcare, where one of two treatment alternatives $a = 1$ or $a' = 0$ are assigned to patients based on their baseline characteristics \vec{C} , in hopes of improving their outcome Y . The dependence of A on \vec{C} would represent *confounding by indication*, a well known issue in observational healthcare data.

Most realistic causal models contain unmeasured confounding variables that introduce spurious dependencies between treatments and outcomes, and complicate causal analysis. For instance, we would expect that in many observational studies the assignment of treatments depends not only on the set of observed baseline characteristics \vec{C} , but also unmeasured characteristics \vec{U} . The resulting model is shown in Fig. 1 (b). Without ad-

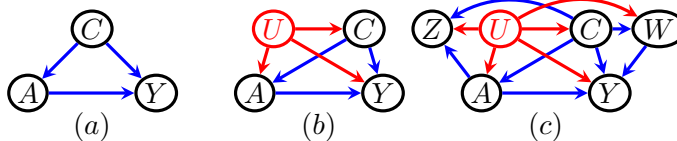


Figure 1: (a) A causal diagram corresponding to the conditionally ignorable model. (b) A causal diagram corresponding to a model where conditional ignorability fails due to the presence of unobserved confounders. (c) A causal diagram corresponding to a model with unobserved confounding where identification of the population ACE is possible via proximal causal inference.

ditional assumptions, the population ACE β is not identified from the observed marginal distribution $p(Y, A, \vec{C})$ in this model (Shpitser and Pearl, 2006a).

A recent line of work (Miao et al., 2018b; Shi et al., 2020; Tchetgen Tchetgen et al., 2020) has developed a new framework of *proximal causal inference* that allows the use of proxy variables to obtain nonparametric identification even in the presence of unobserved confounders.

2.1 An Example Of Proximal Causal Inference

To illustrate how proximal causal inference works, we consider a classical observational study with a point exposure A , an outcome Y , and a set of baseline covariates, some of which are observed (\vec{C}), and others are unobserved (\vec{U}). In this study, exposures are assigned based on values of \vec{C}, \vec{U} , thus the causal relationship of A and Y , as quantified by the average causal effect $\beta \equiv \mathbb{E}[Y(a) - Y(a')]$ is obscured by spurious associations induced by covariates. A causal diagram representing this study is shown in Fig. 1 (b).

Since some of these covariates are not observed, covariate adjustment will not suffice to identify β . Indeed, without further assumptions β is not identified from data obtained from such a study. Proximal causal inference proceeds by assuming that while the vector \vec{U} itself is not observed, there exist observed proxies of \vec{U} . These proxies are subdivided into the control (or treatment-inducing) set which we will call \vec{Z} , and the post-exposure (or outcome-inducing) set, which we will call \vec{W} . Examples of such proxies would include medical tests (ordered both before and after the exposure is assigned) aiming to provide incomplete information about the unobserved course of disease progression in the patients' body.

Both proxies may depend on covariates \vec{C} , the control proxy \vec{Z} may be associated with the exposure A (in our example \vec{Z} is caused by A , but \vec{Z} may also cause A), while the post-exposure proxy \vec{W} may influence the outcome. To enable identification, the control and post-treatment proxies must satisfy a number of independence assumptions. In our example, since the control proxies \vec{Z} are influenced by the exposure A , these assumptions are stated on their counterfactual versions $\vec{Z}(a)$. Specifically, we have:

$$\vec{Z}(a) \perp\!\!\!\perp Y(a) \mid \vec{U}, \vec{C} \text{ for all } a \in \mathfrak{X}_A \quad (1)$$

$$\vec{W} \perp\!\!\!\perp A, \vec{Z}(a) \mid \vec{U}, \vec{C} \quad (2)$$

In addition, the model assumes a version of conditional ignorability and positivity given \vec{C}, \vec{U} :

$$Y(a) \perp\!\!\!\perp A \mid \vec{U}, \vec{C} \text{ for all } a \in \mathfrak{X}_A; \quad p(A \mid \vec{u}, \vec{c}) > 0 \text{ for all } \vec{u} \in \mathfrak{X}_{\vec{U}}, \vec{c} \in \mathfrak{X}_{\vec{C}}. \quad (3)$$

In the interest of conciseness, we will not explicitly mention the positivity assumption in subsequent derivations, and will instead implicitly assume all conditioning events that arise have support. A causal diagram that displays relationships of proxy variables to other variables consistent with the above assumptions is shown in Fig. 1 (c).

Assumptions (1) and (3) imply, by graphoid axioms (Dawid, 1979) and consistency, the following:

$$Y(a) \perp\!\!\!\perp \vec{Z}(a), A \mid \vec{U}, \vec{C} \Rightarrow Y(a) \perp\!\!\!\perp \vec{Z}(a) \mid \vec{U}, \vec{C}, A \Rightarrow Y \perp\!\!\!\perp \vec{Z} \mid \vec{U}, \vec{C}, A. \quad (4)$$

Finally, we assume there exists an *outcome bridge function* $b(Y, \vec{W}, A, \vec{C})$ defined as a solution to the following integral equation (specifically a Fredholm equation of the first kind):

$$p(y|a, \vec{z}, \vec{c}) = \sum_{\vec{w}} b(y, \vec{w}, a, \vec{c}) p(\vec{w}|a, \vec{c}, \vec{z}), \quad (5)$$

where $\sum_{\vec{w}}$ may denote integration for continuous state spaces. If we are interested in only β , it is possible to assume an outcome bridge function $\tilde{b}(\vec{W}, A, \vec{C})$ that is not a function of \vec{Y} and solves the following equation instead:

$$\mathbb{E}[Y|a, \vec{z}, \vec{c}] = \sum_{\vec{w}} \tilde{b}(\vec{w}, a, \vec{c}) p(\vec{w}|a, \vec{c}, \vec{z}).$$

Nevertheless, we will present integral equations for the density, as in (5) to aid subsequent developments. Techniques for solving the integral equations of the form in (5) have been derived in functional analysis; sufficient conditions for existence of a solution are discussed in detail in the context of proximal causal identification in (Miao et al., 2018b; Shi et al., 2020; Tchetgen Tchetgen et al., 2020). Note that it is not necessary to require that the bridge function be unique.

Note in particular that since (2) and (4) hold, the existence of solutions to above equations implies \vec{W} must depend on \vec{U} given \vec{C} , and further \vec{Z} must depend on \vec{U} given \vec{C} and A . This is because if $\vec{W} \perp\!\!\!\perp \vec{U} \mid \vec{C}$, the graphoid axioms imply that $\vec{W} \perp\!\!\!\perp A, \vec{Z}(a), \vec{U} \mid \vec{C}$, and if $\vec{Z} \perp\!\!\!\perp \vec{U} \mid A, \vec{C}$, the graphoid axioms imply $\vec{Z} \perp\!\!\!\perp Y, \vec{U} \mid A, \vec{C}$. Either of these independences further imply the above equations do not admit solutions. Thus, all identification results that rely on existence of solutions of Fredholm equations such as (5) are examples of *generic* identification, and will not hold in all causal models corresponding to the graph in Fig. 1 (c), but only in those models where appropriate dependences hold between unobserved confounders and proxy variables. Note that, similar to the proximal causal models we consider here, the well-established instrumental variable model is likewise a framework for generic identification.

Finally, we assume the following *completeness condition*:

$$\mathbb{E}[v(\vec{U})|\vec{z}, a, \vec{c}] = 0 \text{ for all } \vec{z}, a \text{ and } \vec{c} \text{ if and only if } v(\vec{U}) = 0. \quad (6)$$

This condition accommodates both categorical and continuous confounders \vec{U} . Completeness is a technical condition taught in most foundational courses in theory of statistical inference. Here one may interpret it as a requirement relating the range of U to that of Z

which essentially states that the set of proxies must have sufficient variability relative to variability of U . The condition is easiest understood in the case of categorical U , Z and W , with number of categories d_u , d_z and d_w respectively. In this case, completeness requires that

$$\min(d_z, d_w) \geq d_u \tag{7}$$

which states that Z and W must each have at least as many categories as U . Intuitively, condition (7) states that proximal causal learning can potentially account for unmeasured confounding in the categorical case as long as the number of categories of U is no larger than that of either proxies Z and W . This further provides a rationale for measuring a rich set of baseline characteristics in observational studies as a potential strategy for mitigating unmeasured confounding via the proximal approach we now describe. Additional discussion regarding completeness condition can be found in (Miao et al., 2018b; Shi et al., 2020; Tchetgen Tchetgen et al., 2020).

Given these assumptions, the counterfactual mean $\mathbb{E}[Y(a)]$ (and therefore β) is identified, due to the following derivation that starts with (5):

$$\begin{aligned} p(Y|a, \vec{z}, \vec{c}) &= \sum_{\vec{w}} b(y, \vec{w}, a, \vec{c})p(\vec{w}|a, \vec{c}, \vec{z}) \Rightarrow \text{(by (2), (4), consistency)} \\ \sum_{\vec{u}} p(Y|a, \vec{u}, \vec{c})p(\vec{u}|a, \vec{z}, \vec{c}) &= \sum_{\vec{w}} b(y, \vec{w}, a, \vec{c}) \sum_{\vec{u}} p(\vec{w}|a, \vec{c}, \vec{u})p(\vec{u}|a, \vec{z}, \vec{c}) \Rightarrow \text{(by (6))} \\ p(Y|a, \vec{u}, \vec{c}) &= \sum_{\vec{w}} b(y, \vec{w}, a, \vec{c})p(\vec{w}|a, \vec{c}, \vec{u}) \Rightarrow \text{(by (2))} \\ \sum_{\vec{u}, \vec{c}} p(Y|a, \vec{u}, \vec{c})p(\vec{u}, \vec{c}) &= \sum_{\vec{u}, \vec{c}} \sum_{\vec{w}} b(y, \vec{w}, a, \vec{c})p(\vec{w}|\vec{c}, \vec{u})p(\vec{u}, \vec{c}) \Rightarrow \text{(by (3))} \\ p(Y(a)) &= \sum_{\vec{c}, \vec{w}} b(y, \vec{w}, a, \vec{c})p(\vec{w}, \vec{c}). \end{aligned} \tag{8}$$

The functional in (8) was called the *proximal g-formula* in (Tchetgen Tchetgen et al., 2020). Estimation methods for this functional have been discussed in (Tchetgen Tchetgen et al., 2020).

3. The Proximal Front-Door Criterion

The basic example of proximal causal inference presented in the previous section relies on assumptions that will not always be satisfied in practical applications. For instance, consider the model shown in Fig. 2 (a), which resembles the setting with unobserved confounding shown in Fig. 1 (b), but with an additional complication that the causal relationship of the treatment A and outcome Y is partially mediated by an observed variable M , which may potentially depend on observed covariates \vec{C} .

We now illustrate how additional assumptions may render the ACE parameter $\beta = \mathbb{E}[Y(a) - Y(a')]$ identified in this model. The first assumption we will use is that \vec{M} is a *strong mediator*, or that interventions on A have no effect on Y , provided \vec{M} is also intervened on, or:

$$Y(a, \vec{m}) = Y(\vec{m}) \text{ for all } a, \vec{m}. \tag{9}$$

In addition, we will use the following assumptions:

$$Y(a, \vec{m}) \perp\!\!\!\perp \vec{M}(a) \mid \vec{C} \tag{10}$$

$$Y(\vec{m}) \perp\!\!\!\perp M \mid \vec{C}, A \tag{11}$$

$$\vec{M}(a) \perp\!\!\!\perp A \mid \vec{C}. \tag{12}$$

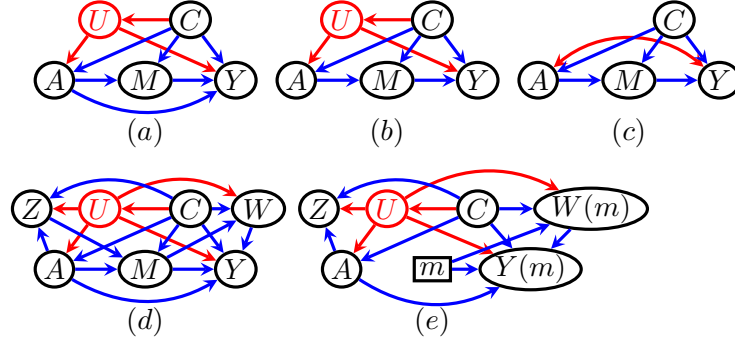


Figure 2: (a) A causal diagram representing a model where non-parametric point identification fails due to the presence of the unobserved common cause of A and Y and the existence of the direct effect of A on Y . (b) A causal diagram representing a model where non-parametric point identification of the population ACE is possible via the front-door criterion of Pearl. (c) A latent projection ADMG of the DAG in (b). (d) A causal diagram representing a model where point identification of the population ACE is impossible non-parametrically, but possible with proximal causal inference methods. (e) A causal diagram representing a world where the mediator variable M is intervened on to value m , resulting in a hypothetical world where proximal causal inference methods may be used to identify $\mathbb{E}[Y(a, m)]$.

These assumptions correspond to a submodel of Fig. 2 (a) shown graphically in Fig. 2 (b). This submodel yields non-parametric identification of $p(Y(a))$ via Pearl's *front-door formula*:

$$p(Y(a)) = \sum_{\vec{c}, \vec{m}} \left(\sum_{\vec{a}} p(Y|\vec{a}, \vec{m}, \vec{c}) p(\vec{a}' | \vec{c}) \right) p(\vec{m}|a, \vec{c}) p(\vec{c}), \quad (13)$$

via the following derivation:

$$\begin{aligned} p(Y(a, \vec{M}(a))) &= \sum_{\vec{m}, \vec{c}} p(Y(a, \vec{m}) | \vec{M}(a) = \vec{m}, \vec{c}) p(\vec{M}(a) = \vec{m} | \vec{c}) p(\vec{c}) \Rightarrow \text{(by (10))} \\ &= \sum_{\vec{m}, \vec{c}} p(Y(a, \vec{m}) | \vec{c}) p(\vec{M}(a) = \vec{m} | \vec{c}) p(\vec{c}) \Rightarrow \text{(by (9))} \\ &= \sum_{\vec{m}, \vec{c}} p(Y(\vec{m}) | \vec{c}) p(\vec{M}(a) = \vec{m} | \vec{c}) p(\vec{c}) \Rightarrow \text{(by (11), (12))} \\ &= \sum_{\vec{m}, \vec{c}} \left(\sum_{\vec{a}'} p(Y|\vec{a}, \vec{m}, \vec{c}) p(\vec{a} | \vec{c}) \right) p(\vec{m}|a, \vec{c}) p(\vec{c}) \end{aligned}$$

The strong mediator assumption (9) is often not realistic in applications, as it implies the analyst is able to find a set of observed variable \vec{M} that completely mediate the effect of A on Y . In settings where finding such a set is unrealistic, the above identification strategy is dubious. An alternative approach to obtaining identification is to use proximal

causal inference. This would entail positing, as in the proximal g-formula shown in (8), a set \vec{Z} of control proxies of \vec{U} , and a set \vec{W} of post-treatment proxies of \vec{U} , resulting in a causal diagram shown in Fig. 2 (d). Note that unlike in (8), the presence of the mediator M prevents assumptions (2) and (4) from holding. Nevertheless, it is possible to obtain identification by noting that if we view \vec{M} as a treatment, it only has observed direct causes, meaning that the effect of \vec{M} on all other variables may be obtained by the g-formula:

$$p^{(\vec{m})}(Y(\vec{m}), \vec{W}(\vec{m}), \vec{Z}, A, \vec{C}) = \sum_{\vec{U}} p(Y, \vec{W}, \vec{C}, \vec{U} | m, A, \vec{Z}) p(A, \vec{Z}) \quad (14)$$

In other words, the interventional distribution $p^{(\vec{m})}$ is identified via a *g-functional* (Robins, 1986), which is a special case of a *Markov kernel* (Lauritzen, 1996), an object that behaves like a conditional distribution but is not necessarily obtained by a conditioning operation. Independence restrictions in $p^{(\vec{m})}$, and thus in the corresponding Markov kernel, may be displayed by the d-separation criterion in a *conditional DAG* shown in Fig. 2 (e), where all arrows into M are removed, and M is made “fixed” (which we denote by a rectangle rather than an ellipse) meaning that it no longer corresponds to a random variable.

It turns out that we can restate assumptions needed for identification that held in the observed data distribution p in Section 2.1 for the kernel $p^{(\vec{m})}$. These independence restrictions can be read off either from Fig. 2 (e), or a generalization described in (Richardson and Robins, 2013). Finally, identifying $p(Y(a))$ from $p^{(\vec{m})}$ immediately yields identification from p , since $p^{(\vec{m})}$ is a function of p given by (14).

Specifically, we have the following analogues of (1) and (2):

$$\vec{Z}(a, \vec{m}) \perp\!\!\!\perp Y(a, \vec{m}) \mid \vec{U}(\vec{m}), \vec{C}(\vec{m}) \quad (15)$$

$$\vec{W}(\vec{m}) \perp\!\!\!\perp A(\vec{m}), \vec{Z}(a, \vec{m}) \mid \vec{U}(\vec{m}), \vec{C}(\vec{m}) \quad (16)$$

as well as a richer set of ignorability type assumptions:

$$Y(\vec{m}), \vec{W}(\vec{m}), \vec{U} \perp\!\!\!\perp \vec{M} \mid A, \vec{C}, \vec{Z} \quad (17)$$

$$Y(a, \vec{m}) \perp\!\!\!\perp \vec{M}(a) \perp\!\!\!\perp A \mid \vec{U}, \vec{C}, \vec{Z}(a) \quad (18)$$

with (18) and consistency implying:

$$Y(a, \vec{m}) \perp\!\!\!\perp A(\vec{m}) \mid \vec{U}(\vec{m}), \vec{C}(\vec{m}), \vec{Z}(a, \vec{m}) \quad (19)$$

and (15), (19) and consistency implying

$$\vec{Z}(\vec{m}) \perp\!\!\!\perp Y(\vec{m}) \mid A(\vec{m}), \vec{U}(\vec{m}), \vec{C}(\vec{m}) \quad (20)$$

We now restate the analogue of the integral equation (5) applicable to the kernel $p^{(\vec{m})}$:

$$p^{(\vec{m})}(Y(\vec{m}) \mid a, \vec{z}, \vec{c}) = \sum_{\vec{w}} b^{(\vec{m})}(Y, \vec{w}, a, \vec{c}, \vec{m}) p^{(\vec{m})}(\vec{W}(\vec{m}) \mid a, \vec{c}, \vec{z}) \quad (21)$$

Finally, we generalize the completeness condition (6) to apply to $p^{(\vec{m})}$ to yield:

$$\mathbb{E}_{p^{(\vec{m})}}[v(\vec{U}) \mid \vec{z}, a, \vec{c}] = 0 \text{ for all } \vec{z}, a, \vec{m}, \text{ and } \vec{c} \text{ if and only if } v(\vec{U}) = 0. \quad (22)$$

Note that the conditional expectation in (22) is a function of \vec{m} , in addition to \vec{z}, a, \vec{c} , since the expectation is with respect to an interventional distribution that depends on \vec{m} .

Armed with these assumptions, we obtain the following derivation (we denote $b^{(m)}(y, \vec{w}, a, \vec{c}, \vec{m})$ by $b^{(m)}$, and $p^{(m)}(Y(\vec{m}) \dots)$ as $p(Y(\vec{m}) \dots)$ for conciseness):

$$\begin{aligned}
 p(Y(\vec{m})|a, \vec{z}, \vec{c}) &= \sum_{\vec{w}} b^{(m)} p(\vec{W}(\vec{m})|a, \vec{c}, \vec{z}) \Rightarrow (\text{by (16), (20)}) \\
 \sum_{\vec{u}} p(Y(\vec{m})|a, \vec{u}, \vec{c}) p(\vec{U}(\vec{m}) = \vec{u}|a, \vec{z}, \vec{c}) &= \sum_{\vec{w}} b^{(m)} \sum_{\vec{u}} p(\vec{W}(\vec{m}) = \vec{w}|a, \vec{u}, \vec{c}) p(\vec{U}(\vec{m}) = \vec{u}|a, \vec{z}, \vec{c}) \Rightarrow (\text{by (22)}) \\
 p(Y(\vec{m})|a, \vec{u}, \vec{c}) &= \sum_{\vec{w}} b^{(m)} p(\vec{W}(\vec{m}) = \vec{w}|a, \vec{u}, \vec{c}) \Rightarrow (\text{by (20), (16)}) \\
 \sum_{\vec{u}} p(Y(\vec{m})|a, \vec{u}, \vec{c}, \vec{z}) p(\vec{U}(\vec{m}) = \vec{u}|\vec{c}, \vec{z}) &= \sum_{\vec{u}} \sum_{\vec{w}} b^{(m)} p(\vec{W}(\vec{m}) = \vec{w}|\vec{u}, \vec{c}, \vec{z}) p(\vec{U}(\vec{m}) = \vec{u}|\vec{c}, \vec{z}) \Rightarrow (\text{by (19)}) \\
 p(Y(a, \vec{m})|\vec{c}, \vec{z}) &= \sum_{\vec{w}} b^{(m)} p(\vec{W}(\vec{m}) = \vec{w}|\vec{c}, \vec{z}) \Rightarrow \\
 \sum_{\vec{m}, \vec{c}, \vec{z}} p(Y(a, \vec{m})|\vec{c}, \vec{z}) p(\vec{m}|a, \vec{c}, \vec{z}) p(\vec{c}, \vec{z}) &= \sum_{\vec{m}, \vec{c}, \vec{z}} \left(\sum_{\vec{w}} b^{(m)} p(\vec{W}(\vec{m})|\vec{c}, \vec{z}) \right) p(\vec{m}|a, \vec{c}, \vec{z}) p(\vec{c}, \vec{z}) \Rightarrow (\text{by (17)}) \\
 \sum_{\vec{m}, \vec{c}, \vec{z}} p(Y(a, \vec{m})|\vec{c}, \vec{z}) p(\vec{m}|a, \vec{c}, \vec{z}) p(\vec{c}, \vec{z}) &= \sum_{\vec{m}, \vec{c}, \vec{z}} \left(\sum_{\vec{w}} b^{(m)} \sum_{\vec{a}} p(\vec{w}|\vec{m}, \vec{a}, \vec{c}, \vec{z}) p(\vec{a}|\vec{c}, \vec{z}) \right) p(\vec{m}|a, \vec{c}, \vec{z}) p(\vec{c}, \vec{z}) \quad (23)
 \end{aligned}$$

For the left hand side in (23), we have, by (10) and consistency:

$$\begin{aligned}
 \sum_{\vec{m}, \vec{c}, \vec{z}} p(Y(a, \vec{m})|\vec{c}, \vec{z}) p(\vec{m}|a, \vec{c}, \vec{z}) p(\vec{c}, \vec{z}) &= \sum_{\vec{m}, \vec{c}, \vec{z}} p(Y(a, \vec{m})|\vec{M}(a) = \vec{m}, \vec{c}, \vec{z}) p(\vec{M}(a) = \vec{m}|\vec{c}, \vec{z}) p(\vec{c}, \vec{z}) \\
 &= p(Y(a, \vec{m})|\vec{M}(a) = \vec{m}) p(\vec{M}(a) = \vec{m}) \\
 &= p(Y(a, \vec{M}(a))) = p(Y(a)).
 \end{aligned}$$

Thus, the model shown in Fig. 2 (d), along with above assumptions, implies the following identification result which we call the *proximal front-door formula*:

$$p(Y(a)) = \sum_{\vec{m}, \vec{c}, \vec{z}} \left(\sum_{\vec{w}} b^{(m)}(y, \vec{w}, a, \vec{c}, \vec{m}) \sum_{\vec{a}} p(\vec{w}|\vec{m}, \vec{a}, \vec{c}, \vec{z}) p(\vec{a}|\vec{c}, \vec{z}) \right) p(\vec{m}|a, \vec{c}, \vec{z}) p(\vec{c}, \vec{z}). \quad (24)$$

We describe an approach to estimating the target parameter identified by (24) in Section 8. We compare this method against baselines defined using the proximal g-formula from (8) and the front-door from (13). By changing our synthetic data distributions, we show that the presence of an $A \rightarrow Y$ edge violates assumption (9) of the front-door method, and that a $Z \rightarrow M \rightarrow W$ path violates assumptions (2) and (4) of the proximal g-formula. These simulations give empirical evidence for the importance of using proximal methods when the assumptions of simpler approaches are violated.

4. The ID Algorithm

General non-parametric identification results, of which the front-door formula (13) is a special case, have been derived using the machinery of graphical causal models, culminating in the characterization of non-parametric identification via the ID algorithm (Tian and Pearl, 2002; Shpitser and Pearl, 2006a; Huang and Valorta, 2006). Here we briefly review this background, prior to introducing a general approach to synthesizing proximal causal inference and non-parametric identification.

The statistical model of a directed acyclic graph (DAG) $\mathcal{G}(\vec{V})$ with a vertex set $\vec{V} \equiv \{V_1, \dots, V_k\}$, called a *Bayesian network*, is the set of distributions that Markov factorize with respect to the DAG as $p(\vec{V}) = \prod_{V_i \in \vec{V}} p(V_i | \text{pa}_{\mathcal{G}}(V_i))$ where $\text{pa}_{\mathcal{G}}(V_i)$ are parents of V_i in \mathcal{G} .

Each variable V_i in a causal model is determined from values of its parents $\text{pa}_{\mathcal{G}}(V_i)$ and an exogenous noise variable ϵ_i via an invariant causal mechanism called a *structural equation* $f_i(\text{pa}_{\mathcal{G}}(V_i), \epsilon_i)$. Causal models allow counterfactual intervention operations, denoted by the $\text{do}(\vec{A})$ operator in (Pearl, 2009). Such operations replace each structural equation $f_i(\text{pa}_{\mathcal{G}}(V_i), \epsilon_i)$ for $V_i \in \vec{A} \subset \vec{V}$ by one that sets V_i to a constant value in \vec{A} corresponding to V_i . The joint distribution of variables in $\vec{Y} \equiv \vec{V} \setminus \vec{A}$ after the intervention $\text{do}(\vec{A})$ was performed is denoted by $p(\vec{Y} \mid \text{do}(\vec{a}))$, equivalently written as $p(\{V_i(\vec{a}) : V_i \in \vec{Y}\})$, or $p(\vec{Y}(\vec{A}))$, where $V_i(\vec{a})$ is a counterfactual random variable or a potential outcome.

A popular causal model called the *non-parametric structural equation model with independent errors (NPSEM-IE)* (Pearl, 2009) assumes, aside from the structural equations for each variable being functions of their parents in the DAG $\mathcal{G}(\vec{V})$, that the joint distribution of all exogenous terms are marginally independent: $p(\epsilon_1, \epsilon_2, \dots) = \prod_{V_i \in \vec{V}} p(\epsilon_i)$. The NPSEM-IE implies the DAG factorization of $p(\vec{V})$ with respect to $\mathcal{G}(\vec{V})$, and a truncated DAG factorization known as the *g-formula*:

$$p(\vec{Y}(\vec{a})) = \prod_{V_i \in \vec{Y}} p(V_i \mid \text{pa}_{\mathcal{G}}(V_i))|_{\vec{A}=\vec{a}} \quad (25)$$

for every $\vec{A} \subseteq \vec{V}$, and $\vec{Y} = \vec{V} \setminus \vec{A}$.

The g-formula (25) provides an elegant link between observed data and counterfactual distributions in causal models where all relevant variables are observed. Causal models that arise in practice, however, contain hidden variables. Representing such models using a DAG $\mathcal{G}(\vec{V} \cup \vec{H})$ where \vec{V} and \vec{H} correspond to observed and hidden variables, respectively, is not very helpful, since applying (25) to $\mathcal{G}(\vec{V} \cup \vec{H})$ results in an expression that involves unobserved variables \vec{H} . A popular alternative is to represent a class of hidden variable DAGs $\mathcal{G}_i(\vec{V} \cup \vec{H}_i)$ by a single *acyclic directed mixed graph* ADMG $\mathcal{G}(\vec{V})$ that contains directed (\rightarrow) and bidirected (\leftrightarrow) edges and no directed cycles via the *latent projection* operation (Verma and Pearl, 1990).

Identification theory of all interventional distributions $p(\vec{Y}(\vec{a}))$ in a hidden variable causal model associated with a DAG $\mathcal{G}(\vec{V} \cup \vec{H})$ may be expressed on the latent projection ADMG $\mathcal{G}(\vec{V})$ without loss of generality.

Under such a causal model, for any disjoint $\vec{A}, \vec{Y} \subseteq \vec{V}$, $p(\vec{Y}(\vec{a}))$ is identified if and only if $p(\vec{Y}^*(\vec{a}))$ is identified, where \vec{Y}^* is the set of ancestors of \vec{Y} in $\mathcal{G}(\vec{V})$ via directed paths not through \vec{A} . The distribution $p(\vec{Y}^*(\vec{a}))$ factorizes with respect to a graph $\mathcal{G}(\vec{V})_{\vec{Y}^*}$, obtained from $\mathcal{G}(\vec{V})$ retaining only vertices in \vec{Y}^* and edges between these vertices. The factorization of $p(\vec{Y}^*(\vec{a}))$ is in terms of a set of interventional distributions associated with bidirected connected sets in $\mathcal{G}(\vec{V})_{\vec{Y}^*}$. These sets are called *districts*, with the set of all districts in $\mathcal{G}(\vec{V})_{\vec{Y}^*}$ denoted by $\mathcal{D}(\mathcal{G}(\vec{V})_{\vec{Y}^*})$.

In particular, we have:

$$p(\vec{Y}(\vec{a})) = \sum_{\vec{Y}^* \setminus \vec{Y}} p(\vec{Y}^*(\vec{a})) = \sum_{\vec{Y}^* \setminus (\vec{Y} \cup \vec{A})} \prod_{\vec{D} \in \mathcal{D}(\mathcal{G}_{\vec{Y}^*})} p(\vec{D} \mid \text{do}(\vec{s}_{\vec{D}})) \quad (26)$$

where $\vec{s}_{\vec{D}}$ are value assignments to $\text{pa}_{\mathcal{G}}(\vec{D}) \setminus \vec{D}$ consistent with \vec{a} .

It is then the case that $p(\vec{Y}(\vec{a}))$ is identified if and only if each term $p(\vec{D} \mid \text{do}(\vec{s}_{\vec{D}}))$ is identified. To check identifiability of $p(\vec{D} \mid \text{do}(\vec{s}_{\vec{D}}))$, we will need to introduce graphs derived from $\mathcal{G}(\vec{V})$ that contains vertices representing random variables, and *fixed* vertices representing intervened on variables. Such graphs are called *conditional ADMGs* or CADMGs,

and represent interventional distributions. The graph in Fig. 2 (e) discussed in Section 3 is a special case of a CADMG.

Given a CADMG $\mathcal{G}(\vec{R}, \vec{S})$, where \vec{R} represent random variables not yet intervened on, and \vec{S} represent former variables that were intervened on, we say $R \in \vec{R}$ is *fixable* if there does not exist another vertex W with a directed path from R to W in $\mathcal{G}(\vec{R}, \vec{S})$ (e.g. W is a descendant of R in $\mathcal{G}(\vec{R}, \vec{S})$) and a bidirected path from R to W . Given a fixable vertex R , a fixing operator $\phi_R(\mathcal{G}(\vec{R}, \vec{S}))$ produces a new CADMG $\mathcal{G}(\vec{R} \setminus \{R\}, \vec{S} \cup \vec{R})$ obtained from $\mathcal{G}(\vec{R}, \vec{S})$ by removing all edges with arrowheads into R . As we describe below, R being fixable in $\mathcal{G}(\vec{R}, \vec{S})$ and the fixing operator yielding $\mathcal{G}(\vec{R} \setminus \{R\}, \vec{S} \cup \vec{R})$ from $\mathcal{G}(\vec{R}, \vec{S})$ is a graphical representation of $p(\vec{R} \setminus \{R\} \mid \text{do}(\vec{s} \cup r))$ being identified from $p(\vec{R} \mid \text{do}(\vec{s}))$ in a particular way.

A sequence $\sigma_{\vec{J}} \equiv \langle J_1, J_2, \dots, J_k \rangle$ of vertices in a set \vec{J} is said to be valid in $\mathcal{G}(\vec{R}, \vec{S})$ if it is either empty, or J_1 is fixable in $\mathcal{G}(\vec{R}, \vec{S})$, and $\tau(\sigma_{\vec{J}}) \equiv \langle J_2, \dots, J_k \rangle$ (the *tail* of the sequence) is valid in $\phi_{J_1}(\mathcal{G}(\vec{R}, \vec{S}))$. Any two distinct sequences $\sigma_{\vec{J}}^1, \sigma_{\vec{J}}^2$ on the same set \vec{J} valid in $\mathcal{G}(\vec{R}, \vec{S})$ yield the same graph: $\phi_{\sigma_{\vec{J}}^1}(\mathcal{G}(\vec{R}, \vec{S})) = \phi_{\sigma_{\vec{J}}^2}(\mathcal{G}(\vec{R}, \vec{S}))$. We will thus write $\phi_{\vec{J}}(\mathcal{G}(\vec{R}, \vec{S}))$ to denote this graph.

Each term $p(\vec{D} \mid \text{do}(\vec{s}_{\vec{D}}))$ in (26) is identified from $p(\vec{V})$ if and only if there exists a sequence $\langle J_1, \dots \rangle$ of elements in $\vec{J} \equiv \vec{V} \setminus \vec{D}$ valid in $\mathcal{G}(\vec{V})$. If such a sequence exists, it implies the following identifying assumptions. Let $\vec{R}_1 = \text{de}_{\mathcal{G}(\vec{V})}(J_1) \setminus \{J_1\}$, and $\vec{T}_1 = \vec{V} \setminus (\vec{R}_1 \cup \{J_1\})$. Similarly, let $\vec{R}_k = \text{de}_{\phi_{\{J_1, \dots, J_{k-1}\}}(\mathcal{G}(\vec{V}))}(J_k) \setminus \{J_k\}$ and $\vec{T}_k = \vec{V} \setminus (\{J_1, \dots, J_{k-1}, J_k\} \cup \vec{R}_k)$, where $\text{de}_{\mathcal{G}}(R_k)$ is the set of descendants of R_k (including R_k itself by convention) in \mathcal{G} . Then, the existence of a valid sequence for $\langle J_1, \dots \rangle$ implies the following assumptions:

$$\vec{R}_1(j_1) \perp\!\!\!\perp J_1 \mid \vec{T}_1 \text{ for all } j_1 \quad (27)$$

$$\vec{R}_k(j_1, \dots, j_k) \perp\!\!\!\perp J_k(j_1, \dots, j_{k-1}) \mid \vec{T}_k(j_1, \dots, j_{k-1}) \text{ for all } j_1, \dots, j_k. \quad (28)$$

Given (27) and (28), we obtain identification of $p(\vec{D} \mid \text{do}(\vec{s}_{\vec{D}}))$ by the following inductive formula:

$$\begin{aligned} p(\vec{V} \setminus \{J_1\} \mid \text{do}(j_1)) &= \frac{p(\vec{V} \setminus \{J_1\}, j_1)}{p(j_1 \mid \vec{T}_1)} = \frac{p(\vec{V} \setminus \{J_1\}, j_1)}{p(j_1 \mid \text{mb}_{\mathcal{G}(\vec{V})}^*(J_1))} \\ p(\vec{V} \setminus \{J_1, \dots, J_k\} \mid \text{do}(j_1, \dots, j_k)) &= \frac{p(\vec{V} \setminus \{J_1, \dots, J_k\}, j_k \mid \text{do}(j_1, \dots, j_{k-1}))}{p(j_k \mid \vec{T}_k, \text{do}(j_1, \dots, j_{k-1}))} \\ &= \frac{p(\vec{V} \setminus \{J_1, \dots, J_k\}, j_k \mid \text{do}(j_1, \dots, j_{k-1}))}{p(j_k \mid \text{mb}_{\phi_{\{J_1, \dots, J_{k-1}\}}(\mathcal{G}(\vec{V}))}^*(J_k), \text{do}(j_1, \dots, j_{k-1}))}, \end{aligned} \quad (29)$$

where for any $J_i \in \vec{R} \setminus \{J_1, \dots, J_{i-1}\}$, $\text{mb}_{\mathcal{G}(\vec{R}, \{J_1, \dots, J_{i-1}\})}^*(J_i)$ denotes all random vertices that are either parents of J_i , or that are connected to J_i via collider paths (paths where all consecutive triplets have arrowheads meeting at the middle vertex). The operations on the right hand side of (29) may be viewed as distributional analogues of the graphical fixing operation ϕ .

As a simple example, we illustrate how identifiability of counterfactuals in Fig. 2 (b) given in (13) may be reformulated in terms of (26) and (29). The latent projection ADMG of the hidden variable DAG in Fig. 2 (b), sometimes called the *front-door graph*, is shown in Fig. 2(c). If we aim to identify $p(Y(a))$ in Fig. 2 (c), we note that $Y^* = \{Y, M, C\}$, with districts in \mathcal{G}_{Y^*} being $\{Y\}, \{M\}, \{C\}$. In fact, valid sequences exists for all sets of elements

outside these districts. Thus, we have the following derivation for the term $p(C|\text{do}(a, y, m))$:

$$\begin{aligned} p(C, A, M|\text{do}(y)) &= \frac{p(C, A, M, y)}{p(y|C, A, M)} \\ p(C, A|\text{do}(y, m)) &= \frac{p(C, A, m|\text{do}(y))}{p(m|A, C, \text{do}(y))} = \frac{p(C, A, m)}{p(m|A, C)} \\ p(C|\text{do}(a, y, m)) &= \frac{p(C, a|\text{do}(y, m))}{p(a|C, \text{do}(y, m))} = \frac{p(C, a)}{p(a|C)} = p(C), \end{aligned}$$

the following derivation for the term $p(M|\text{do}(a, y, c))$:

$$\begin{aligned} p(C, A, M|\text{do}(y)) &= \frac{p(C, A, M, y)}{p(y|C, A, M)} \\ p(C, M|\text{do}(y, a)) &= \frac{p(C, a, M|\text{do}(y))}{p(a|C, \text{do}(y))} = \frac{p(C, a, M)}{p(a|C)} \\ p(M|\text{do}(y, a, c)) &= \frac{p(c, M|\text{do}(y, a))}{p(c|\text{do}(y, a))} = \frac{p(M|a, c)p(c)}{p(c)} = p(M|a, c), \end{aligned}$$

and the following derivation for the term $p(Y|\text{do}(a, m, c))$:

$$\begin{aligned} p(A, M, Y|\text{do}(c)) &= \frac{p(c, A, M, Y)}{p(c)} \\ p(A, Y|\text{do}(c, m)) &= \frac{p(A, m, Y|\text{do}(c))}{p(m|A, \text{do}(c))} = \frac{p(A, m, Y|c)}{p(m|A, c)} \\ p(Y|\text{do}(c, m, a)) &= \frac{p(a, Y|\text{do}(c, m))}{p(a|Y, \text{do}(c, m))} = \frac{p(Y|m, a, c)p(a|c)}{\sum_{\tilde{a}} p(Y|m, \tilde{a}, c)p(\tilde{a}|c)} = \sum_{\tilde{a}} p(Y|m, \tilde{a}, c)p(\tilde{a}|c). \end{aligned}$$

We then conclude that $p(Y(a))$ is identified from $p(C, A, M, Y)$ via (26) and (29) by

$$\sum_{m,c} p(Y|\text{do}(a, m, c))p(m|\text{do}(a, y, c))p(c|\text{do}(a, y, m)) = \sum_{m,c} \left(\sum_{\tilde{a}} p(Y|m, \tilde{a}, c)p(\tilde{a}|c) \right) p(m|a, c)p(c).$$

The expectation of this functional taken with respect to Y yields (13).

5. The Proximal ID Algorithm

The ID algorithm is complete for non-parametric identification of interventional distributions $p(\vec{Y}(\vec{a}))$ in causal models represented by any hidden variable DAG $\mathcal{G}(\vec{V} \cup \vec{H})$, for any disjoint $\vec{Y}, \vec{A} \subseteq \vec{V}$. The distribution $p(\vec{Y}(\vec{a}))$ is not identified whenever one or more of the terms $p(\vec{D} | \text{do}(\vec{s}_{\vec{D}}))$ in (26) cannot be obtained from $p(\vec{V})$. This, in turn, happens whenever no valid sequence for $\vec{V} \setminus \vec{D}$ exists in $\mathcal{G}(\vec{V})$. A variable generally fails to be fixable in the latent projection due to an excessive number of latent variables in the underlying hidden variable DAG.

For example, the distribution $p(Y(a))$ is not identified in the hidden variable causal model shown in Fig. 3 (a). This is because \mathcal{G}_{Y^*} obtained from the latent projection of this model, shown in Fig. 3 (b) contains a single district $\{Y\}$, and the set $\vec{V} \setminus \{Y\} = \{C, M, A\}$ does not have a valid sequence in Fig. 3 (b).

However, assume we could observe U , but not H or L . $p(Y(a))$ would be identified in the resulting graph, shown in Fig. 3 (c) since the sequence $\langle M, U, C, A \rangle$ is now valid,

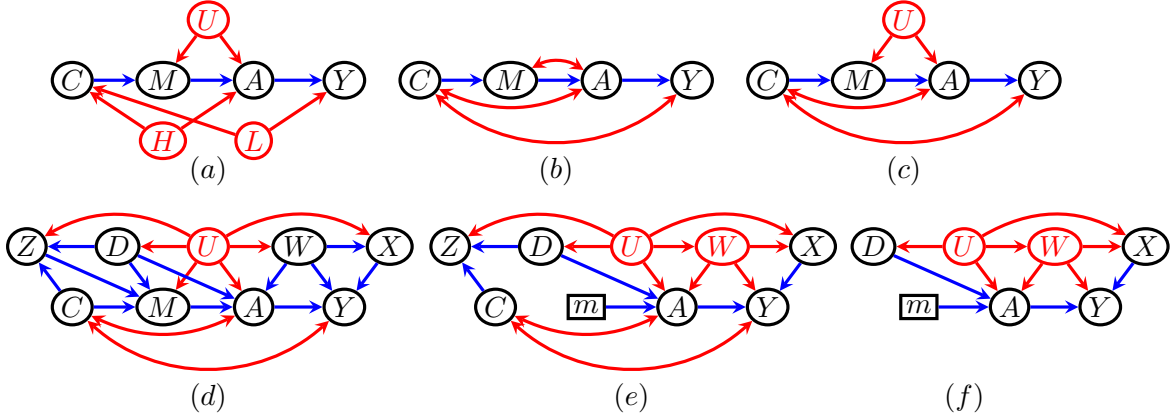


Figure 3: (a) A hidden variable DAG where $p(Y(a))$ is not identified from $p(C, M, A, Y)$. (b) A latent projection ADMG of the DAG in (a). (c) A partial latent projection where the variable U permits identification, provided it is observed. (d) A partial latent projection where the variable U is hidden, but proximal causal inference using variables Z, D, W and X allow identification. (e) A conditional graph representing the situation where M is intervened to value m , identified by using the proxy W , prior to using the proxy X to obtain identification by marginalizing C and intervening on A .

yielding:

$$\begin{aligned}
 p(Y, U, C, A | \text{do}(m)) &= \frac{p(Y, m, U, C, A)}{p(m | U, C)} = p(Y, A | m, U, C) p(U, C) \\
 p(Y, C, A | \text{do}(m, u)) &= \frac{p(Y, u, C, A | \text{do}(m))}{p(u | \text{do}(m))} = \frac{p(Y, A | m, u, C) p(u, C)}{p(u)} = p(Y, A | m, u, C) p(C | u) \\
 p(Y, A | \text{do}(m, u, c)) &= \frac{p(Y, c, A | \text{do}(m, u))}{p(c | A, Y, \text{do}(m, u))} = \frac{p(Y, A | m, u, c) p(c | u)}{\sum_c p(Y, A | m, u, c) p(c | u)} \\
 p(Y | \text{do}(m, u, c, a)) &= \frac{p(Y, a | \text{do}(m, u, c))}{p(a | \text{do}(m, u, c))} = \frac{\frac{p(Y, a | m, u, c) p(c | u)}{\sum_c p(Y, a | m, u, c) p(c | u)}}{\sum_y \frac{p(y, a | m, u, c) p(c | u)}{\sum_c p(y, a | m, u, c) p(c | u)}} = p(Y(a)). \tag{30}
 \end{aligned}$$

Note that fixing operations above depend on observing U .

If U is not observed, it may be possible instead to use techniques from proximal causal inference to account for it, for the purposes of the fixing operation. Note that whenever a particular variable is fixed, that variable is viewed as a “treatment,” and all variables that remain random at that fixing step are viewed as “outcomes.”

To proceed, we will assume, as before, the existence of two control proxies Z and D , and two post-treatment proxies W and X . The first proxy W views M as a “treatment,” and A, Y, X , jointly as an outcome. The second proxy X views A as a “treatment,” and Y as an “outcome.” Proxies Z and D will be used to solve the integral equations involving W and X , respectively.

We now describe generalizations of assumptions we used in previous examples that allow *recursive* identification using either proximal causal inference, or the fixing operation

from the ID algorithm. We first consider analogues of (1) and (2):

$$A(m), Y(m) \perp\!\!\!\perp Z \mid U, C, D, X \quad (31)$$

$$W \perp\!\!\!\perp M, Z \mid U, C, D, X \quad (32)$$

Next, we assume the analogue of conditional ignorability (3):

$$A(m), Y(m) \perp\!\!\!\perp M \mid U, C, D, Z, X \quad (33)$$

Here the variable M to be fixed is viewed as a treatment and descendant variables of M , namely A and Y , are viewed as outcomes.

Further, we will assume the existence of a bridge function. Specifically, we have:

$$p(y, a \mid m, z, c, d, x) = \sum_w b_1(y, a, x, w, m, d, c) p(w \mid m, c, d, z, x), \quad (34)$$

and a slight extension of the completeness condition (6):

$$\mathbb{E}[v(U) \mid z, m, c, d, x] = 0 \text{ for all } z, m, c, x \text{ and } d \text{ if and only if } v(U) = 0. \quad (35)$$

Assumptions (31) and (33) imply, by graphoid axioms and consistency:

$$A(m), Y(m) \perp\!\!\!\perp Z, M \mid U, C, D, X \Rightarrow A(m), Y(m) \perp\!\!\!\perp Z \mid M, U, C, D, X \Rightarrow A, Y \perp\!\!\!\perp Z \mid U, C, M, D, X \quad (36)$$

We then have the following derivation, where we will denote $b_1(y, a, x, w, m, d, c)$ by b_1 :

$$\begin{aligned} p(y, a \mid m, z, c, d, x) &= \sum_w b_1 p(w \mid m, c, d, z, x) \Rightarrow \text{(by (36), (32))} \\ \sum_u p(y, a \mid m, c, d, x, u) p(u \mid m, z, c, d, x) &= \sum_w b_1 \sum_u p(w \mid m, c, d, x, u) p(u \mid m, z, c, d, x) \Rightarrow \text{(by (35))} \\ p(y, a \mid m, c, d, x, u) &= \sum_w b_1 p(w \mid m, c, d, x, u) \Rightarrow \text{(by (32), (36))} \\ \sum_u p(y, a \mid m, c, d, u, z, x) p(u, c, d, z, x) &= \sum_u \sum_w b_1 p(w \mid c, d, x, u, z) p(u, c, d, z, x) \Rightarrow \text{(by (33))} \\ p(y, a, x, c, d, z \mid \text{do}(m)) &= p(Y(m) = y, A(m) = a, x, c, d, z) = \sum_w b_1 p(w, c, d, z, x). \end{aligned} \quad (37)$$

The resulting interventional distribution corresponds to the graph shown in Fig. 3 (e). Given that proximal causal inference was used to intervene on M , variables Z and C can now be intervened on, since they are both fixable in Fig. 3 (e). In fact, these operations correspond to marginalizations in $p(y, a, x, c, d, z \mid \text{do}(m))$, yielding a new distribution $p(y, a, x, d \mid \text{do}(m)) = \sum_{w, c, z} b_1(y, a, x, w, m, d, c) p(w, c, d, z) = \sum_{w, c} b_1(y, a, x, w, m, d, c) p(w, c, d)$, and the corresponding graph Fig. 3 (f).

Note that in this graph, the proxy variable W , which was previously used to identify the joint response $Y(m), A(m), X$ of intervening on M , has been marginalized via the integral equation (34), and thus *itself* serves as an unobserved confounder creating a spurious association between the subsequent variable we want to fix, namely A , and the variable which we want to treat as “the outcome,” namely Y , in the world where M was intervened on to value m , and Z and C had been summed out.

However, we can now invoke proximal causal identification recursively by appealing to the existence of proxy variables X and D that allow us to adjust for the presence of W .

We require variants of proximal assumptions used in the previous step, but applicable to the distribution $p(y, a, x, d|\text{do}(m))$ corresponding to the current step.

The assumptions that serve as analogues of (31) and (32) are:

$$D \perp\!\!\!\perp Y(m, a)|W, U \quad (38)$$

$$X \perp\!\!\!\perp A(m), D|W, U \quad (39)$$

Next, we assume a generalized version of ignorability:

$$Y(a, m) \perp\!\!\!\perp A(m) | W, D, U \quad (40)$$

Further, we assume the existence of a second bridge function. Specifically, we have:

$$p(Y(m) = y|A(m) = a, d) = \sum_x b_2(y, x, a)p(x|A(m) = a, d). \quad (41)$$

Note that distributions $p(Y(m)|A(m), D)$ and $p(X|A(m), D)$ appearing in this integral equation are functionals of $p(Y(m) = y, A(m) = a, X, C, D)$, which is identified by (37).

We will assume, in addition, the following completeness condition:

$$\mathbb{E}_{p^{(m)}}[v(W, U)|a, d] = 0 \text{ for all } a \text{ and } d \text{ if and only if } v(W, U) = 0, \quad (42)$$

where the expectation is taken with respect to $p^{(m)}(W, U|A(m) = a, D)$.

Assumptions (38) and (40) imply, by graphoid axioms and consistency:

$$Y(a, m) \perp\!\!\!\perp D, A(m)|W, U \Rightarrow Y(a, m) \perp\!\!\!\perp D|A(m), W, U \Rightarrow Y(m) \perp\!\!\!\perp D|A(m), W, U \quad (43)$$

Given these assumptions, we obtain the following derivation, where we will denote $b_2(y, x, a)$ by b_2 :

$$\begin{aligned} p(Y(m) = y|A(m) = a, d) &= \sum_x b_2 p(x|A(m) = a, d) \Rightarrow \text{(by (43), (39))} \\ \sum_{w,u} p(Y(m) = y|A(m) = a, w, u)p(w, u|a, d) &= \sum_x b_2 \sum_{w,u} p(x|A(m) = a, w, u)p(w, u|a, d) \Rightarrow \text{(by (42))} \\ p(Y(m) = y|A(m) = a, w, u) &= \sum_x b_2 p(x|A(m) = a, w, u) \Rightarrow \text{(by (39), (43))} \\ \sum_{w,u,d} p(Y(m) = y|A(m) = a, w, u, d)p(w, u, d) &= \sum_{w,u} \sum_{x,d} b_2 p(x|w, u, d)p(w, u, d) \Rightarrow \text{(by (40))} \\ p(Y(m, a)) &= p(Y(a)) = \sum_{x,d} b_2(y, x, a)p(x, d) = \sum_x b_2(y, x, a)p(x). \end{aligned}$$

This yields the following identification result:

$$\begin{aligned} p(Y(a)) &= \sum_x b_2(y, x, a)p(x), \text{ where } b_2 \text{ is obtained via} \quad (44) \\ p(Y(m) = y|A(m) = a, d) &= \sum_x b_2(y, x, a)p(x|A(m) = a, d), \text{ which is equivalent to} \\ \frac{\sum_{w,x,c} b_1(y, a, x, w, m, c, d)p(w, c, d, x)}{\sum_{w,x,c,y} b_1(y, a, x, w, m, c, d)p(w, c, d, x)} &= \sum_x b_2(y, x, a) \frac{\sum_{w,y,c} b_1(y, a, x, w, m, c, d)p(w, c, d, x)}{\sum_{w,y,c,x} b_1(y, a, x, w, m, c, d)p(w, c, d, x)}, \\ &\text{and } b_1 \text{ is obtained via} \\ p(y, a|m, z, c, d, x) &= \sum_w b_1(y, a, x, w, m, d, c)p(w|m, c, d, z, x). \end{aligned}$$

Note that the functional for $p(Y(a))$ is not a function of m , although it may appear to depend on m if we examine the syntactic form of (44). In particular, we might expect b_2 that solves the integral equation in the second line to depend on the value of m in the corresponding interventional distributions in that equation. However, b_2 does not, in fact depend on the value of m under the model in Fig. 3 (d). This fact corresponds to the generalized independence (“Verma”) restriction implied by the model in Fig. 3 (d).

It is instructive to consider the structural similarities of expressions in (44) and (30). The functional in (30) was obtained by fixing M , and conditioning on u and c , and finally applying the definition of conditioning to the resulting object to obtain $p(Y|\text{do}(m, u, c, a))$. The functional in (44) was obtained by fixing M using proximal inference to deal with unobserved confounding between M and its causal descendants, which explains the appearance of the first bridge function b_1 in the functional. Afterwards, variables Z and C are marginalized out, and then subsequent fixing had to be performed using a recursive application of proximal inference, with another set of proxy variables, and another bridge function b_2 . In other words, the fixing sequence that gave rise to (30) is $\langle M, U, C, A \rangle$, while the fixing sequence that gave rise to (44) is $\langle M, Z, C, A, X, D \rangle$, with M and A not being fixed in the “conventional way,” but with the aid of proxies and bridge functions. The similarity of the fixing sequences leads to the structural similarity of resulting functionals, just as the proximal g-formula resembles ordinary g-formula, and the proximal front-door functional (24) resembles the ordinary front-door functional (13).

5.1 The General Case

We will now consider general identification theory in hidden variable DAG causal models that combines ideas from the ID algorithm and proximal inference, and that generalizes all examples discussed in the previous sections. We appropriately name the resulting algorithm the *proximal ID algorithm*.

We will consider hidden variable DAGs with two types of hidden variables: those that are “unresolvable,” and those that are “resolvable” using proximal inference. We will denote the former types of hidden variables by \vec{L} , the latter by \vec{U} , and observed variables by \vec{V} as before. Given a hidden variable DAG $\mathcal{G}(\vec{V} \cup \vec{U} \cup \vec{L})$, we will formulate our theory using a hidden variable ADMG $\mathcal{G}(\vec{V} \cup \vec{U})$ obtained by a latent projection operation applied only to \vec{L} .

As we saw in examples in previous sections, proximal inference proceeds using a set of post-treatment proxies which are subsequently marginalized, due to being involved in integral equations. As a result, our formulation of the proximal ID algorithm will use a subset $\vec{M} \subseteq \vec{V}$ as post-treatment proxies, and treat them *as if they were unobserved* when defining the district factorization used in the algorithm.

Given an ADMG $\mathcal{G}(\vec{V} \cup \vec{U})$, and disjoint $\vec{A}, \vec{Y} \subseteq \vec{V}$, fix $\vec{M} \subseteq \vec{V} \setminus (\vec{Y} \cup \vec{A})$, and let $\vec{V}^* \equiv \vec{V} \setminus \vec{M}$. We start with the following factorization:

$$p(\vec{Y}(\vec{a})) = \sum_{\vec{Y}^* \setminus \vec{Y}} \prod_{\vec{D} \in \mathcal{D}(\mathcal{G}(\vec{V}^*)_{\vec{Y}^*})} p(\vec{D}|\text{do}(\vec{s}_{\vec{D}})), \tag{45}$$

where \vec{Y}^* is the set of ancestors of \vec{Y} in $\mathcal{G}(\vec{V}^*)$ via directed paths that do not intersect \vec{A} , and $\vec{s}_{\vec{D}}$ are value assignments to $\text{pa}_{\mathcal{G}}(\vec{D}) \setminus \vec{D}$ consistent with \vec{a} . Note that the districts in the above factorization are defined with respect to a subgraph of $\mathcal{G}(\vec{V}^*)$, where both \vec{U} and \vec{M} are “projected out.”

To obtain identification, we must ensure that each term $p(\vec{D}|\text{do}(\vec{s}_{\vec{D}}))$ is identified from $p(\vec{V})$ by a combination of regular fixing operations and proximal inference steps. To this

end, we formulate a set of conditions where a particular treatment variable $A \in \vec{V}$ may be fixed either in the usual way as done by the ID algorithm, or by using proximal inference. Both kinds of steps are formulated in a hidden variable conditional ADMG (CADMG) $\mathcal{G}(\vec{V} \cup \vec{M} \cup \vec{U}, \vec{W})$, where \vec{W} represent variables previously fixed, \vec{U} represents unobserved variables that remain relevant in the problem (e.g. have more than one child in $\vec{V} \cup \vec{M}$), \vec{M} represents post-treatment proxies available for use, and \vec{V} represents all other observed variables. This CADMG will represent a corresponding interventional distribution $p(\vec{v}, \vec{m}, \vec{u} | \text{do}(\vec{w}))$. Note that the algorithm does not have access to this entire distribution, but only certain marginals that suffice for proximal inference.

Specifically, there exists a subset $\vec{V}_1 \subseteq \vec{V}$ and (possibly overlapping) $\vec{M}_1, \vec{M}_2 \subseteq \vec{M}$ such that $\vec{M}_1 \cup \vec{M}_2 = \vec{M}$, and the algorithm has access to $p(\vec{v}_1, \vec{m}_1 | \text{do}(\vec{w}))$, and $p(\vec{v}, \vec{m}_2 | \text{do}(\vec{w}))$. We can view the set \vec{M}_1 as those proxy variables that have possibly been used for proximal causal inference steps, but remain available for setting up subsequent integral equations, provided only variables in \vec{V}_1 are used. We call the distribution $p(\vec{v}_1, \vec{m}_1 | \text{do}(\vec{w}))$ the *reusing margin*. Variables in \vec{M}_2 are proxy variables that have not previously been used, and we call the distribution $p(\vec{v}, \vec{m}_2 | \text{do}(\vec{w}))$ containing remaining observed variables, along with proxies \vec{M}_2 the *inductive margin*. During initial steps of the algorithm, both inductive and reusing margins are initialized as $p(\vec{v} \cup \vec{m})$. We now describe the inductive operation of the algorithm with both the ordinary fixing operation, and with proximal inference steps.

5.1.1 THE PROXIMAL ID ALGORITHM: THE ORDINARY FIXING STEP

For $A \in \vec{V}$, if A is fixable in $\mathcal{G}(\vec{V} \cup \vec{M}_2, \vec{W})$ (obtained as a latent projection from $\mathcal{G}(\vec{V} \cup \vec{M} \cup \vec{U}, \vec{W})$), we obtain a new CADMG $\phi_A(\mathcal{G}(\vec{V} \cup \vec{M} \cup \vec{H}, \vec{W})) = \tilde{\mathcal{G}}((\vec{V} \cup \vec{M} \cup \vec{H}) \setminus \{A\}, \vec{W} \cup \{A\})$ (since it is the case that if A is fixable in $\mathcal{G}(\vec{V} \cup \vec{M}_2, \vec{W})$, it is also fixable in $\mathcal{G}(\vec{V} \cup \vec{M} \cup \vec{H}, \vec{W})$ (Richardson et al., 2017)). The new distribution corresponding to this CADMG is $p(\vec{v} \setminus \{a\}, \vec{m}, \vec{u} | \text{do}(\vec{w}, a))$, where the inductive margin $p(\vec{v} \setminus \{a\}, \vec{m}_2 | \text{do}(\vec{w}, a))$ is available using the usual fixing operation on distributions applied to $p(\vec{v}, \vec{m}_2 | \text{do}(\vec{w}))$.

Specifically, if A is fixable, we have the following identity, mirroring (29):

$$p(\vec{V} \setminus \{A\}, \vec{M}_2 | \text{do}(\vec{w}, a)) = \frac{p(\vec{V} \setminus \{A\}, \vec{M}_2, a | \text{do}(\vec{w}))}{p(a | \text{mb}_{\mathcal{G}(\vec{V} \cup \vec{M}_2, \vec{W})}^*(A), \text{do}(\vec{w}))}, \quad (46)$$

where, as before, $\text{mb}_{\mathcal{G}(\vec{V} \cup \vec{M}_2, \vec{W})}^*(A)$ denotes all random vertices that are either parents of A , or that are connected to A via collider paths (paths where all consecutive triplets have arrowheads meeting at the middle vertex).

In addition, if $A \in \vec{V}_1$ and A is fixable in $\mathcal{G}(\vec{V}_1 \cup \vec{M}_1, \vec{W})$, we obtain the reusing margin $p(\vec{v}_1 \setminus \{a\}, \vec{m}_1 | \text{do}(\vec{w}, a))$ for subsequent steps, by the usual fixing operation. Specifically, we have:

$$p(\vec{V}_1 \setminus \{A\}, \vec{M}_1 | \text{do}(\vec{w}, a)) = \frac{p(\vec{V}_1 \setminus \{A\}, \vec{M}_1, a | \text{do}(\vec{w}))}{p(a | \text{mb}_{\mathcal{G}(\vec{V}_1 \cup \vec{M}_1, \vec{W})}^*(A), \text{do}(\vec{w}))}.$$

If $A \notin \vec{V}_1$ or A is not fixable in $\mathcal{G}(\vec{V}_1 \cup \vec{M}_1, \vec{W})$, we obtain the reusing margin $p(\vec{v}'_1, \vec{m}'_1 | \text{do}(\vec{w}, a))$, where $\vec{V}'_1 = \vec{V}_1 \setminus \text{de}_{\mathcal{G}(\vec{V} \cup \vec{M} \cup \vec{U}, \vec{W})}(A)$, and $\vec{M}'_1 = \vec{M}_1 \setminus \text{de}_{\mathcal{G}(\vec{V} \cup \vec{M} \cup \vec{U}, \vec{W})}(A)$, for subsequent steps, by marginalization:

$$p(\vec{v}'_1, \vec{m}'_1 | \text{do}(\vec{w}, a)) = p(\vec{v}'_1, \vec{m}'_1 | \text{do}(\vec{w})) = \sum_{\vec{v}_1 \setminus \vec{v}'_1, \vec{m}_1 \setminus \vec{m}'_1} p(\vec{v}_1, \vec{m}_1 | \text{do}(\vec{w})),$$

provided \vec{V}'_1, \vec{M}'_1 are non-empty.

5.1.2 THE PROXIMAL ID ALGORITHM: THE PROXIMAL INFERENCE STEP

Given an inductive margin $p(\vec{v}, \vec{m}_2 | \text{do}(\vec{w}))$, and a reusing margin $p(\vec{v}_1, \vec{m}_1 | \text{do}(\vec{w}))$ identified after an intervention $\text{do}(\vec{w})$, fix $A \in \vec{V}$ where we aim to identify inductive and reusing margins given an intervention $\text{do}(\vec{w}, a)$. To this end we define a subset $\vec{M}^* \subseteq \vec{M}$ of post-treatment proxies (where A is the treatment), and define $\vec{R} \equiv \text{de}_{\mathcal{G}(\vec{V} \cup (\vec{M}_2 \setminus \vec{M}^*), \vec{W})}(A) \setminus \{A\}$ (note that we latent project $(\vec{M} \setminus \vec{M}_2) \cup \vec{M}^* \cup \vec{H}$ from the CADMG associated with the current step before defining \vec{R}), and $\vec{T} \equiv (\vec{V} \cup \vec{M}_2) \setminus (\vec{R} \cup \vec{M}^*)$.

To apply proximal inference to identify the effect of the intervention on A on the remaining variables in the inductive margin, we assume there exists $\vec{U}^* \subseteq \vec{U}$, $\vec{Z} \subseteq \vec{T}$ such that the following set of conditions hold:

$$(\{A\} \cup \vec{T}) \not\subseteq \vec{V}_1 \Rightarrow \vec{M}^* \subseteq \vec{M}_2; (\{A\} \cup \vec{T}) \subseteq \vec{V}_1 \Rightarrow (\vec{M}^* \subseteq \vec{M}_1 \vee \vec{M}^* \subseteq \vec{M}_2) \quad (47)$$

$$\text{de}_{\mathcal{G}(\vec{V} \cup \vec{U}^*, \vec{W})}(A) \cap \text{dis}_{\mathcal{G}(\vec{V} \cup \vec{U}^*, \vec{W})}(A) = \{A\}, \quad (48)$$

$$\vec{R}(a) \perp\!\!\!\perp \vec{Z}(a) | \vec{U}^*, \vec{T} \setminus \vec{Z} \quad (49)$$

$$\vec{M}^* \perp\!\!\!\perp A, \vec{Z}(a) | \vec{U}^*, \vec{T} \setminus \vec{Z} \quad (50)$$

$$\vec{R}(a) \perp\!\!\!\perp A | \vec{T}, \vec{U}^* \quad (51)$$

$$p(\vec{r}^a | a, \vec{t}, \text{do}(w)) = \sum_{\vec{m}^*} b_A(\vec{m}^*, \vec{r}, a, \vec{t} \setminus \vec{z}, \vec{w}) p(\vec{m}^* | a, \vec{t}, \text{do}(\vec{w})) \text{ for a bridge function } b_A(\vec{m}^*, \vec{r}, a, \vec{t}, \vec{w}) \quad (52)$$

$$\sum_{\vec{U}^*} v(\vec{U}^*) p(\vec{U}^* | a, \vec{t}, \text{do}(\vec{w})) = 0 \text{ for all } a, \vec{t}, \vec{w} \text{ if and only if } v(\vec{U}^*) = 0, \quad (53)$$

where all conditions hold in $p(\vec{v}, \vec{m}, \vec{h} | \text{do}(\vec{w}))$, and (48) implies (51) under the causal model associated with the graph from which $\mathcal{G}(\vec{V} \cup \vec{M} \cup \vec{H}, \vec{W})$ was recursively derived. In fact, (47) implies that the integral equation in (52) is a function of the inductive margin, or the inductive and reusing margins.

If the above conditions are satisfied, we proceed by a general version of derivations described in the previous sections. We first note that assumptions (49) and (51), together with the graphoid axioms and consistency, imply:

$$\vec{R}(a) \perp\!\!\!\perp \vec{Z}(a), A | \vec{U}^*, \vec{T} \setminus \vec{Z} \Rightarrow \vec{R}(a) \perp\!\!\!\perp \vec{Z}(a) | A, \vec{U}^*, \vec{T} \setminus \vec{Z} \Rightarrow \vec{R} \perp\!\!\!\perp \vec{Z} | A, \vec{U}^*, \vec{T} \setminus \vec{Z}. \quad (54)$$

We then get the following derivation, where we denote $b_A(\vec{m}, \vec{r}, a, \vec{t}, \vec{w})$ by b_A for conciseness:

$$\begin{aligned}
 p(\vec{r}|a, \vec{t}, \text{do}(\vec{w})) &= \sum_{\vec{m}^*} b_A p(\vec{m}^*|a, \vec{t}, \text{do}(\vec{w})) \Rightarrow (\text{by (50), (54), consistency}) \\
 \sum_{\vec{u}^*} p(\vec{r}|\vec{u}^*, a, \vec{t} \setminus \vec{z}, \text{do}(\vec{w})) p(\vec{u}^*|a, \vec{t}, \text{do}(\vec{w})) &= \sum_{\vec{m}^*} b_A \sum_{\vec{u}^*} p(\vec{m}^*|a, \vec{t} \setminus \vec{z}, \vec{u}^*, \text{do}(\vec{w})) p(\vec{u}^*|a, \vec{t}, \text{do}(\vec{w})) \Rightarrow (\text{by (53)}) \\
 p(\vec{r}|\vec{u}^*, a, \vec{t} \setminus \vec{z}, \text{do}(\vec{w})) &= \sum_{\vec{m}^*} b_A p(\vec{m}^*|a, \vec{t} \setminus \vec{z}, \vec{u}^*, \text{do}(\vec{w})) \Rightarrow (\text{by (50), (54)}) \\
 \sum_{\vec{u}^*} p(\vec{r}|\vec{u}^*, a, \vec{t}, \text{do}(\vec{w})) p(\vec{u}^*, \vec{t}|\text{do}(\vec{w})) &= \sum_{\vec{u}^*} \sum_{\vec{m}^*} b_A p(\vec{m}^*|\vec{t}, \vec{u}^*, \text{do}(\vec{w})) p(\vec{u}^*, \vec{t}|\text{do}(\vec{w})) \Rightarrow (\text{by (51)}) \\
 \sum_{\vec{u}^*} \frac{p(\vec{r}, \vec{t}, \vec{u}^*, a|\text{do}(\vec{w}))}{p(a|\vec{t}, \vec{u}^*, \text{do}(\vec{w}))} &= p(\vec{r}, \vec{t}|\text{do}(\vec{w}, a)) = \sum_{\vec{m}^*} b_A p(\vec{m}^*, \vec{t}|\text{do}(\vec{w})) \tag{55}
 \end{aligned}$$

This derivation yields the inductive margin $p(\vec{r}, \vec{t}|\text{do}(\vec{w}, a))$ for the next step, which potentially includes elements in \vec{M}_2 in \vec{T} . To obtain the reusing margin $p(\vec{v}_1, \vec{m}_1|\text{do}(\vec{w}))$ we follow precisely the steps in the previous subsection. Note that the inductive margin always marginalizes out the proxies \vec{M}^* that were used in the current step of the algorithm, while the reusing margins aims to keep these proxies in the problem, if possible.

The application of proximal causal inference above may be viewed as creating a new subproblem from $\mathcal{G}(\vec{V} \cup \vec{M}_2 \cup \vec{U}, \vec{W})$ by fixing A , and viewing \vec{M}^* as unobserved variables. We thus extend the fixing operator $\phi(\cdot)$ to apply to $\mathcal{G}(\vec{V} \cup \vec{M} \cup \vec{U}, \vec{W})$, even if A is not fixable in $\mathcal{G}(\vec{V} \cup \vec{M}_2, \vec{W})$ as was required in the previous subsection, provided that above conditions are satisfied for $\mathcal{G}(\vec{V} \cup \vec{M} \cup \vec{U}, \vec{W})$, and the inductive and reusing margins, given A and a set \vec{M}^* .

To obtain identification of every term $p(\vec{D}|\text{do}(\vec{s}_{\vec{D}}))$ in (45), we need to apply fixing operations and proximal causal inference inductively to the set $\vec{V} \setminus \vec{D}$. We thus generalize the definition of a valid sequence in the ID algorithm as follows. Given a CADMG $\mathcal{G}(\vec{V} \cup \vec{M} \cup \vec{H}, \vec{W})$, and the corresponding inductive and reusing margins, a sequence $\sigma = \langle Z_1, Z_2, \dots \rangle$ is said to be admissible if either σ is empty, or $\tau(\sigma)$ is admissible in $\phi_{Z_1}(\mathcal{G}(\vec{V} \cup \vec{M} \cup \vec{H}, \vec{W}))$, and either Z_1 is fixable in $\mathcal{G}(\vec{V} \cup \vec{M}_2, \vec{W})$ or there is a set $\vec{M}^* \subseteq \vec{M}$ such that conditions (47), (48), (49), (50), (51), (52), (53) apply to A and \vec{M}^* , given $\mathcal{G}(\vec{V} \cup \vec{M} \cup \vec{H}, \vec{W})$, the inductive margin $p(\vec{v}, \vec{m}_2|\text{do}(\vec{w}))$, and the reusing margin $p(\vec{v}_1, \vec{m}_1|\text{do}(\vec{w}))$.

We are now ready to state the proximal ID algorithm formally. Fix an ADMG $\mathcal{G}(\vec{V} \cup \vec{U})$, with disjoint $\vec{A}, \vec{Y} \subseteq \vec{V}$, fix $\vec{M} \subseteq \vec{V} \setminus (\vec{A} \cup \vec{Y})$, $\vec{V}^* \equiv \vec{V} \setminus \vec{M}$, and \vec{Y}^* is the set of ancestors of \vec{Y} in $\mathcal{G}(\vec{V}^*)$ via directed paths that do not intersect \vec{A} .

Then $p(\vec{Y}(\vec{a}))$ is identified from $p(\vec{V})$ in the causal model represented by $\mathcal{G}(\vec{V} \cup \vec{U})$ given the proxy set \vec{M} if for every $\vec{D} \in \mathcal{D}(\mathcal{G}(\vec{V}^*)_{\vec{Y}^*})$, the sequence $\vec{V}^* \setminus \vec{D}$ is admissible in $\mathcal{G}(\vec{V} \cup \vec{U}, \vec{W})$. Furthermore, we then have

$$p(\vec{Y}(\vec{a})) = \sum_{\vec{Y}^* \setminus \vec{Y}} \prod_{\vec{D} \in \mathcal{D}(\mathcal{G}(\vec{V}^*)_{\vec{Y}^*})} p(\vec{D}|\text{do}(\vec{s}_{\vec{D}})),$$

with every $p(\vec{D}|\text{do}(\vec{s}_{\vec{D}}))$ identified inductively via (55) and (46).

Theorem 5.1 *The proximal ID algorithm is sound.*

Proof First, note that standard causal models of a hidden variable DAG $\mathcal{G}(\vec{V} \cup \vec{H})$ imply that every interventional distribution, including $p(\vec{Y}^*(\vec{a}))$, district factorizes with respect to the district in the corresponding induced subgraph $\mathcal{G}(\vec{V})_{\vec{Y}^*}$ of the latent projection ADMG

$\mathcal{G}(\vec{V})$) of $\mathcal{G}(\vec{V} \cup \vec{H})$. The conclusion then follows inductively (on the fixing sequence of every term) from the soundness of the ID algorithm (see e.g. the proof in (Richardson et al., 2017)), and the derivation yielding (55). ■

5.1.3 A NOTE ON CHARACTERIZATION OF IDENTIFICATION BY PROXIMAL CAUSAL INFERENCE METHODS

The ID algorithm yields a total identification result, meaning that whenever it successfully returns an identifying functional for $p(\vec{Y}(\vec{a}))$, this functional equals to the parameter of interest anywhere in the causal model represented by the input graph \mathcal{G} . This fact allowed prior work (Shpitser and Pearl, 2006a; Huang and Valtorta, 2006) to show that the ID algorithm is *complete*¹, meaning that whenever it fails, the target parameter is not identified in the model.

By contrast, the proximal ID algorithm yields a generic identification result, meaning that a function output by the algorithm can only be obtained in a subset of the model represented by the graph where the appropriate Fredholm equations yield solutions. Historically, it has proven to be very challenging to derive completeness results for generic identification algorithms – the problem remains open even in the simple case of linear Gaussian causal models. Thus, the question of whether the proximal ID algorithm is complete is currently open.

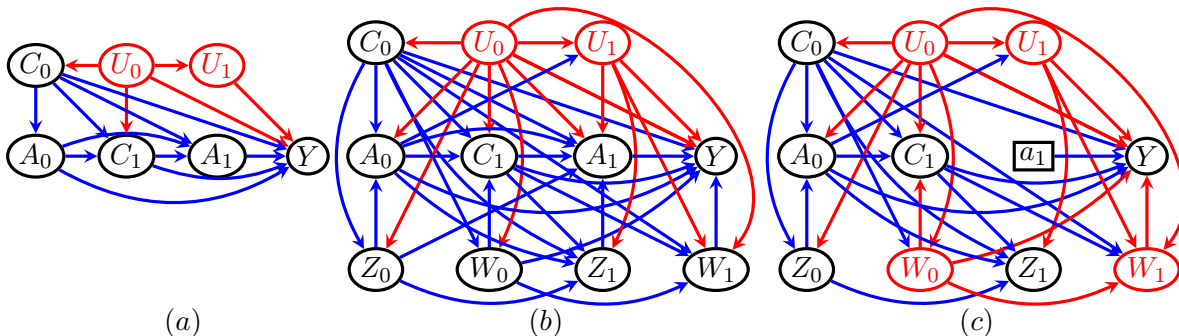


Figure 4: (a) A causal diagram corresponding to the sequentially ignorable model, where $p(Y(a_0, a_1))$ is identified via the g-computation algorithm. (b) A causal diagram corresponding to the proximal generalization of the sequentially ignorable model. (c) A causal diagram obtained from (b) after the treatment A_1 is fixed using proximal causal inference with the post-treatment proxy W_1 .

1. Note that this is a different notion of completeness from the completeness assumption discussed earlier, and is instead more closely related to the notion of soundness and completeness of deductive systems.

6. An Important Special Case: The Proximal G-Computation Algorithm

Here we consider an important special case of the proximal ID algorithm that arises in longitudinal studies, where treatments are administered sequentially over time. If the policy assigning treatments at each time point in such a study was based only on the past observed variables, the resulting causal model is the well known *sequentially ignorable model* where identification is achieved by means of the g-computation algorithm (Robins, 1986). An example of such a model is shown in Fig. 4 (a), where we have

$$p(Y(a_0, a_1) = y) = p(y|\text{do}(a_0, a_1)) = \sum_{c_0, c_1} p(y|a_0, c_0, a_1, c_1)p(c_1|a_0, c_0)p(c_0). \quad (56)$$

If the policy assigning treatments at each time point also depends on unobserved variables, the distribution $p(Y(a_0, a_1))$ is not identified non-parametrically. However, provided the appropriate post-treatment, and control proxies exist, we can exploit the proximal ID algorithm to obtain identification. Consider the model shown in Fig. 4 (b), where we are interested in identifying $p(Y(a_0, a_1))$.

Here identification proceeds in two stages, with both reusing and inductive margins initialized as $p(y, \bar{c}, \bar{a}, \bar{z}, \bar{w})$. For the first stage, we make the following assumptions, implied by the graphical causal model, in addition to the bridge integral equation, and a completeness condition:

$$Y(a_1) \perp\!\!\!\perp Z_0, Z_1 \mid U_0, U_1, A_0, C_0, C_1 \quad (57)$$

$$W_1, W_0 \perp\!\!\!\perp A_1, Z_0, Z_1 \mid U_0, U_1, A_0, C_0, C_1 \quad (58)$$

$$Y(a_1) \perp\!\!\!\perp A_1 \mid Z_0, Z_1, U_0, U_1, A_0, C_0, C_1 \quad (59)$$

$$p(y|a_1, z_0, a_0, c_0, w_0, c_1, z_1) = \sum_{w_1, w_0} b_{A_1}(w_1, y, a_1, z_0, a_0, c_0, w_0, c_1)p(w_1, w_0|a_1, z_0, a_0, c_0, c_1, z_1)$$

$$\text{for a bridge function } b_{A_1}(w_1, y, a_1, z_0, a_0, c_0, w_0, c_1) \quad (60)$$

$$\sum_{U_1} p(v(U_1)|a_1, z_0, a_0, c_0, w_0, c_1, z_1) = 0 \text{ for all } a_1, z_0, a_0, c_0, w_0, c_1, z_1 \text{ if and only if } v(U_1) = 0. \quad (61)$$

We note that (57) and (59), together with the graphoid axioms and consistency, imply:

$$\begin{aligned} Y(a_1) \perp\!\!\!\perp Z_0, Z_1, A_1 \mid U_0, U_1, A_0, C_0, C_1 &\Rightarrow Y(a_1) \perp\!\!\!\perp Z_0, Z_1 \mid A_1, U_0, U_1, A_0, C_0, C_1 \\ &\Rightarrow Y \perp\!\!\!\perp Z_0, Z_1 \mid A_1, U_0, U_1, A_0, C_0, C_1 \end{aligned} \quad (62)$$

Let $\bar{z} = (z_0, z_1)$, $\bar{c} = (c_0, c_1)$, $\bar{a} = (a_0, a_1)$, $\bar{w} = (w_0, w_1)$, $\bar{u} = (u_0, u_1)$. Then we have:

$$p(y|\bar{a}, \bar{z}, \bar{c}) = \sum_{\bar{w}} b_{A_1}p(\bar{w}|\bar{a}, \bar{z}, \bar{c}) \Rightarrow \text{(by (58), (62))}$$

$$\sum_{\bar{u}} p(y|\bar{a}, \bar{c}, \bar{u})p(\bar{u}|\bar{a}, \bar{z}, \bar{c}) = \sum_{\bar{w}} b_A \sum_{\bar{u}} p(\bar{w}|\bar{a}, \bar{c}, \bar{u})p(\bar{u}|\bar{a}, \bar{z}, \bar{c}) \Rightarrow \text{(by (61))}$$

$$p(y|\bar{a}, \bar{c}, \bar{u}) = \sum_{\bar{w}} b_{AP}p(\bar{w}|\bar{a}, \bar{c}, \bar{u}) \Rightarrow \text{(by (58), (62))}$$

$$\sum_{\bar{u}} p(y|\bar{a}, \bar{z}, \bar{c}, \bar{u})p(\bar{u}, a_0, \bar{z}, \bar{c}) = \sum_{\bar{u}} \sum_{\bar{w}} b_{AP}p(\bar{w}|a_0, \bar{z}, \bar{c}, \bar{u})p(\bar{u}, a_0, \bar{z}, \bar{c}) \Rightarrow \text{(by (59))}$$

$$\sum_{\bar{u}} \frac{p(y, \bar{a}, \bar{z}, \bar{c}, \bar{u})}{p(a_1|\bar{u}, \bar{c}, \bar{z}, a_0)} = p(y, a_0, \bar{z}, \bar{c}|\text{do}(a_1)) = \sum_{\bar{w}} b_{AP}p(\bar{w}, a_0, \bar{z}, \bar{c}).$$

This results in the graph in Fig. 4 (b), and identification of the reusing margin $p(y, a_0, \bar{z}, \bar{c} | \text{do}(a_1))$. Since A_1 is not fixable in $\mathcal{G}(\vec{C}, \vec{A}, \vec{Z}, \vec{W}, Y)$, we obtain the reusing margin by marginalizing out descendants of A_1 , yielding $p(\bar{c}, a_0, \bar{z}, \bar{w})$.

Since Z_1 has no descendants once A_1 is fixed, the variable may be safely marginalized out from both margins, yielding:

$$\begin{aligned} p(y, a_0, z_0, \bar{c} | \text{do}(a_1)) &= \sum_{\bar{w}} b_{AP}(\bar{w}, a_0, z_0, \bar{c}) \\ p(\bar{c}, a_0, z_0, \bar{w}) &= \sum_{z_1} p(\bar{c}, a_0, \bar{z}, \bar{w}). \end{aligned}$$

We employ the following assumptions for the second stage, which consist of independences implied by the causal model, a bridge integral equation, and a completeness condition:

$$Y(a_1, a_0), C_1(a_1, a_0) \perp\!\!\!\perp Z_0 \mid U_0, C_0 \quad (63)$$

$$W_0 \perp\!\!\!\perp A_0, Z_0 \mid U_0, C_0 \quad (64)$$

$$Y(a_1, a_0), C_1(a_1, a_0) \perp\!\!\!\perp A_0 \mid Z_0, U_0, C_0 \quad (65)$$

$$\begin{aligned} p(y, c_1 | a_0, z_0, c_0, \text{do}(a_1)) &= \sum_{w_0} b_{A_0}(w_0, y, c_1, a_0, c_0, a_1) p(w_0 | a_0, z_0, c_0) \\ &\text{for a bridge function } b_{A_0}(w_0, y, c_1, a_0, c_0, a_1) \end{aligned} \quad (66)$$

$$\sum_{U_0} p(v(U_0) | a_0, z_0, c_0, \text{do}(a_1)) = 0 \text{ for all } z_0, a_0, c_0, a_1 \text{ if and only if } v(U_0) = 0, \quad (67)$$

where the left hand side of (66) is a function of the inductive margin obtained from the first stage, and the right hand side of (66) is a function of the reusing margin obtained from the first stage.

We note that (63) and (65), together with the graphoid axioms and consistency, imply:

$$\begin{aligned} Y(a_1, a_0), C_1(a_1, a_0) \perp\!\!\!\perp Z_0, A_0 \mid U_0, C_0 &\Rightarrow Y(a_1, a_0), C_1(a_1, a_0) \perp\!\!\!\perp Z_0 \mid A_0, U_0, C_0 \\ &\Rightarrow Y(a_1), C_1 \perp\!\!\!\perp Z_0 \mid A_0, U_0, C_0 \end{aligned} \quad (68)$$

We then obtain the following derivation for the second stage:

$$p(y, c_1 | a_0, z_0, c_0, \text{do}(a_1)) = \sum_{w_0} b_{A_0} p(w_0 | a_0, z_0, c_0) \Rightarrow \text{(by (64), (68))} \quad (69)$$

$$\sum_{u_0} p(y, c_1 | u_0, a_0, c_0, \text{do}(a_1)) p(u_0 | a_0, z_0, c_0) = \sum_{w_0} b_{A_0} \sum_{u_0} p(w_0 | a_0, u_0, c_0) p(u_0 | a_0, z_0, c_0) \Rightarrow \text{(by (67))} \quad (70)$$

$$p(y, c_1 | u_0, a_0, c_0, \text{do}(a_1)) = \sum_{w_0} b_{A_0} p(w_0 | a_0, u_0, c_0) \Rightarrow \text{(by (64), (68))} \quad (71)$$

$$\sum_{u_0} p(y, c_1 | u_0, a_0, z_0, c_0, \text{do}(a_1)) p(u_0 | c_0, z_0, \text{do}(a_1)) = \sum_{u_0} \sum_{w_0} b_{A_0} p(w_0 | u_0, z_0, c_0) p(u_0 | c_0, z_0) \Rightarrow \text{(by (65))} \quad (72)$$

$$\sum_{u_0} \frac{p(y, c_1, u_0, a_0, z_0, c_0 | \text{do}(a_1))}{p(a_0 | c_0, z_0, u_0, \text{do}(a_1))} = p(y, c_1, z_0, c_0 | \text{do}(a_1, a_0)) = \sum_{w_0} b_{A_0} p(w_0, z_0, c_0). \quad (73)$$

Together, the above two derivations imply the following identification result:

$$\begin{aligned}
 p(y|\text{do}(a_1, a_0)) &= \sum_{w_0, c_1, c_0} b_{A_0} p(w_0, c_0), \text{ where } b_{A_0} \text{ is solved for via} \\
 p(y, c_1|a_0, z_0, c_0, \text{do}(a_1)) &= \sum_{w_0} b_{A_0}(w_0, y, c_1, a_0, c_0, a_1) p(w_0|a_0, z_0, c_0), \text{ where} \\
 p(y, c_1|a_0, z_0, c_0, \text{do}(a_1)) &= \frac{\sum_{\bar{w}} b_{AP}(\bar{w}, a_0, z_0, \bar{c})}{\sum_{y, c_1, \bar{w}} b_{AP}(\bar{w}, a_0, z_0, \bar{c})}, \text{ since} \\
 p(y, a_0, z_0, \bar{c}|\text{do}(a_1)) &= \sum_{\bar{w}} b_{AP}(\bar{w}, a_0, z_0, \bar{c}).
 \end{aligned}$$

This section provides a graphical description of the proximal g-computation algorithm first described in (Tchetgen Tchetgen et al., 2020). We note a few differences between the algorithm in this section, and the one in (Tchetgen Tchetgen et al., 2020). First, the target of inference in (Tchetgen Tchetgen et al., 2020) was a counterfactual expectation, and thus all derivations employed integral equations on the expectation scale. Second, control proxies Z_1 and Z_0 , while used in the same way in both versions of the algorithm, were immediately removed in (Tchetgen Tchetgen et al., 2020) upon use. In our version of the algorithm, they are kept around after their use, and are subsequently removed by means of the fixing operation. This step was made explicit to emphasize the connection between the proximal ID algorithm, and the (classical) ID algorithm.

Finally, the assumptions employed in the second stage of the derivation in (Tchetgen Tchetgen et al., 2020) were formulated on potential outcomes derived from Y_1 , rather than on the joint potential outcomes derived from Y_1 and C_1 as is done here. This is possible because the marginalization over C_1 can be performed earlier in the algorithm while retaining validity of the overall derivation. The advantage of formulating assumptions only on Y_1 becomes apparent in high dimensional applications, where the bridge integral equation becomes much easier to formulate if fewer variables are involved. In this paper, the marginalization over C_1 is performed at the end of the algorithm, to better illustrate the connection with the operation of the (classical) ID algorithm. A general method for performing summations in a way that results in lower dimensional integral equations is closely related to methods for efficient marginalization in graphical models via *sum product algorithms*, and is left to future work.

7. Relationship to Identification of Responses to Counterfactual Policies

Consider an ADMG $\mathcal{G}(\vec{V} \cup \vec{U})$ representing a hidden variable DAG model (where \vec{U} are “resolvable” hidden variables). Given a set of treatments \vec{A} , denote a set of non-descendants \vec{W}_A for every $A \in \vec{A}$. Given an outcome Y , and a set of known functions (or policies) $\vec{f}_{\vec{A}} \equiv \{f_A : \mathfrak{X}_{\vec{W}_A} \mapsto \mathfrak{X}_A : A \in \vec{A}\}$, define $Y(\vec{f}_{\vec{A}})$ as

$$Y(\{A \leftarrow f_A(\vec{W}_A(\vec{f}_{\vec{A}})) : A \in \vec{A} \cap \text{pa}_{\mathcal{G}(\vec{V} \cup \vec{U})}(Y)\}, \{W(\vec{f}_{\vec{A}}) : W \in \text{pa}_{\mathcal{G}(\vec{V} \cup \vec{U})}(Y) \setminus \vec{A}\}).$$

As an example, in Fig. 4 (a), given functions $\vec{f}_{\{A_0, A_1\}} \equiv \{f_{A_0} : \mathfrak{X}_{C_0} \mapsto \mathfrak{X}_{A_0}; f_{A_1} : \mathfrak{X}_{\{C_0, C_1\}} \mapsto \mathfrak{X}_{A_1}\}$,

$$Y(\vec{f}_{\{A_0, A_1\}} \equiv Y(C_0, A_0 \leftarrow f_{A_0}(C_0), C_1(C_0, A_0 \leftarrow f_{A_0}(C_0)), A_1 \leftarrow f_{A_1}(C_0, C_1(C_0, A_0 \leftarrow f_{A_0}(C_0)))).$$

This counterfactual outcome represents response of Y had values of A_0 and A_1 been set, possibly contrary to fact, to outputs of functions f_{A_0} and f_{A_1} (which themselves possibly take counterfactual responses to these functions as inputs). Counterfactuals of this sort arise in precision medicine, analysis of complex longitudinal studies, and reinforcement learning. An important identification question is whether such responses are identified.

Formally, given an ADMG $\mathcal{G}(\vec{V} \cup \vec{U})$, a set of treatments \vec{A} , a subset $\vec{W}_A \subseteq \vec{V} \setminus \vec{A}$ of non-descendants of A for each $A \in \vec{A}$, a set of policies $\vec{f}_{\vec{A}} \equiv \{f_A : \mathfrak{X}_{\vec{W}_A} \mapsto \mathfrak{X}_A : A \in \vec{A}\}$, and a set of outcomes $\vec{Y} \subseteq \vec{V} \setminus \vec{A}$, the question is whether $p(\vec{Y}(\vec{f}_{\vec{A}}))$ is identified from $p(\vec{V})$.

A general identification algorithm for this problem was proposed in (Tian, 2008), and proven complete (for the unrestricted policy class) in (Shpitser and Sherman, 2018). In fact, this algorithm reduced the problem of identification of responses to policies to the problem of identification of joint responses to ordinary interventions. Specifically, $p(\vec{Y}(\vec{f}_{\vec{A}}))$ is identified if and only if $p(\vec{Y}(\vec{a}), \{\vec{W}_A(\vec{a}) : A \in \vec{A}\})$ is identified. Moreover, since identification is insensitive to specific values \vec{a} of intervened-on treatments, the former counterfactual distribution $p(\vec{Y}(\vec{f}_{\vec{A}}))$ may be readily expressed as a marginal of the latter, as follows: $\sum_{\{\vec{w}_A : A \in \vec{A}\}} p(\vec{Y}(\{A \leftarrow f_A(\vec{w}_A) : A \in \vec{A}\}, \{\vec{W}_A(\vec{a}) = \vec{w}_A : A \in \vec{A}\}))$. This suggests that the proximal ID algorithm can be readily adapted for identification of responses to policies, essentially without change.

8. Simulations

We now turn to an array of simulation studies to demonstrate how the identifying assumptions of the proximal ID algorithm can enable unbiased estimation. We focus on the DAG in Figure 2(d) to highlight how simpler baseline methods fail when their assumptions are violated. While the identification theory allows for U, C, Z, W , and M to be vectors, our simulations is restricted to the univariate case for simplicity, so vector superscripts are dropped from the notation that follows. The full details of how we parameterize the synthetic datasets we consider are in Section 8.3. Our code implementing our methods and generating our datasets is included as a supplement.

8.1 Proximal Front-Door Estimator

Equation (24) provides the identifying functional for the DAG in Figure 2(d). Our estimator from this functional proceeds in the following steps. First, we estimate a propensity score model for M , $p(M | A, Z, C)$. Using this model to weight² the observed data distribution gives us the kernel $p^{(m)}$ from Equation (14), which we use to estimate the bridge function $b^{(m)}(Y | w, a, c, m)$. Following Miao et al. (2018b), we estimate this function using generalized method of moments (GMM).

Once we have the bridge function $b^{(m)}$, we learn a propensity model for A , $p(A | Z, C)$ and a regression model for W , $E_{(m)}[W | A, Z, C]$. Then, using the observed Z_i and C_i from each row of our observed data matrix, we sample 100 trajectories of $Y(a = 1)$ and $Y(a = 0)$ as defined in Equation (24). We then return our estimate of the causal effect as the average over $Y(1) - Y(0)$ for all sampled trajectories and all data rows.

8.2 Baseline Methods

To comprehensively benchmark the performance of our proximal front-door estimator, we compare to several other methods for estimating the causal effect of A on Y .

2. We truncate weights at the 2.5th and 97.5th percentiles.

Oracle Baseline A motivating assumption for this work is that the unobserved confounder U makes impossible non-parametric identification of the causal effect. If U were in fact observed, the causal effect could be estimated with a simple application of the g-formula which adjusts for the confounding effect of Z , U , and C (Robins, 1986). While our methods are designed for when U is unobserved, comparing against an oracle with access to U lower-bounds the estimation error for a given dataset and sample size.

Naive Front-Door In Figure 2(d), the direct effect of A on Y makes the causal effect unidentified by the classic front-door estimator given by Equation (13). The front-door estimator relies on the assumption that $M \perp U \mid A$, which is violated in Figure 2(d), so we expect this estimator to return biased estimates of the causal effect whenever there is a nonzero direct effect of A on Y . In the “**Varied $A \rightarrow Y$ Effect**” experiments below, we specifically explore how the bias of this estimator changes as we vary the coefficient responsible for this direct effect.

Simple Proximal In Figure 1(c), the causal effect of A on Y is identified using proximal inference. In particular, Equation (8) provides the identifying functional, which relies on assumptions (1 - 6). In Figure 2(d), assumptions (1) and (2) are violated by the existence of M and the path $Z \rightarrow M \rightarrow W$. Our Simple Proximal baseline uses the identifying functional from (8), ignoring the violation of these assumptions. We expect this estimator to produce biased estimates of the causal effect whenever there is a nonzero effect along the $Z \rightarrow M \rightarrow W$ path. In the “**Varied $Z \rightarrow M \rightarrow W$ Effect**” experiments below, we explore how the bias of this estimator changes as we vary the coefficients responsible for this path-specific effect. Our implementation of this method draws from the code released by Miao et al. (2018b).

8.3 Synthetic Data

The choices made in designing a simulation study can heavily influence the apparent results (Gentzel et al., 2019). By releasing our code, evaluating over several randomly-sampled DGPs and datasets, and exploring violations of our method’s assumptions, we strive to make our simulation studies as reproducible and extensible as possible.

We make several simplifications for our simulation studies. We only consider univariate U, C, Z, W , and M . We consider settings in which Z and M are either both binary and or both Gaussian; otherwise, A is always binary and all other variables are always Gaussian. All effects in the DGP are linear without interaction terms.

For each of the below experiments, all results are an average of 256 evaluations; we sample 64 datasets from each of four DGPs. The coefficients of the four DGPs are randomly sampled from $\text{Unif}(-2, 2)$ and each dataset is sampled with a different random seed. For the below experiments in which we alter one or two coefficients of the DGP to explore violations of different assumptions, we do so before sampling the dataset but leave all other coefficients as is.

For all experiments, we compare each method’s estimate of the causal effect against the true effect as computed analytically from the underlying parameters of the DGP. In the tables below, “Mean Absolute Bias” and “Percent Absolute Bias” refer to the following

Metric	Mean Absolute Bias			Percent Absolute Bias		
	4000	16000	64000	4000	16000	64000
Sample Size						
Oracle Backdoor	0.007	0.003	0.002	0.007	0.003	0.001
Naive Front-Door	1.003	1.005	1.003	0.790	0.791	0.789
Simple Proximal	1.655	1.661	1.669	1.116	1.119	1.127
Proximal Front-Door	0.006	0.009	0.004	0.005	0.008	0.003

Table 1: **Varied Sample Size** experiments. Each cell of the table shows the metrics in (74) and (75) aggregated over four DGPs and 64 datasets per DGP. Z and M are Gaussian.

computations:

$$\text{Mean Absolute Bias} = \frac{1}{N_1} \sum_{i=1}^{N_1} \left| \frac{1}{N_2} \sum_{j=1}^{N_2} (\hat{\beta}_{i,j} - \beta_i) \right| \quad (74)$$

$$\text{Percent Absolute Bias} = \frac{1}{N_1} \sum_{i=1}^{N_1} \frac{1}{|\beta_i|} \left| \frac{1}{N_2} \sum_{j=1}^{N_2} (\hat{\beta}_{i,j} - \beta_i) \right| \quad (75)$$

where $N_1 = 4$ is the number of DGPs and $N_2 = 64$ is the number of datasets on which we evaluate. $\hat{\beta}_{i,j}$ is the method’s estimate of the causal effect for DGP i and dataset j , and β_i is the true causal effect for that DGP. Note the absolute value inside the summation over DGPs in (74) and (75). This is important because we sample our DGP parameters from $\text{Unif}(-2, 2)$, which is mean zero. Because the effects in our DGP are linear without interactions, the biases of the naive front-door is dependent on the sign and magnitude of the coefficient controlling the $A \rightarrow Y$ edge that violates its assumptions. Thus if we average over many DGPs, that coefficient may be approximately mean zero and the bias may disappear, even if the method has high bias for any single DGP. We further explore how specific coefficient values affect the behavior of the different estimators in Tables 2, 3, and 4.

8.4 Experiments

Varied Sample Size We first demonstrate how each method converges as we increase the sample size. Table 1 shows these results when Z and M are Gaussian. We see both the backdoor oracle and proximal front-door quickly converge towards zero bias. The proximal front-door estimator achieves bias close to the oracle, highlighting the effectiveness of proximal methods for recovering from unobserved confounding. Neither naive front-door nor the simple proximal estimators converge towards zero bias as the sample size increases.

Varied $A \rightarrow Y$ Effect We then examine how the direct effect of $A \rightarrow Y$ empirically introduces bias to the naive front-door estimator. For each of the four DGPs we consider, we modify the parameters of the sampling distribution by changing the $A \rightarrow Y$ coefficient to a value $\beta_{AY} \in \{0, 0.2, 0.4, 0.8\}$. For each value β_{AY} , we sample 256 datasets of 4000 samples.

Table 2 shows the coverage and interval width of these methods when we use non-parametric bootstrap with 64 resamplings to produce a 95% confidence interval. We see

Metric	Bootstrap Interval Coverage				Bootstrap Interval Width			
	0	0.2	0.4	0.8	0	0.2	0.4	0.8
$A \rightarrow Y$								
Oracle Backdoor	0.938	0.938	0.938	0.938	0.338	0.338	0.338	0.338
Naive Front-Door	0.766	0.219	0.020	0.000	0.258	0.254	0.251	0.245
Simple Proximal	0.000	0.000	0.000	0.000	0.694	0.693	0.694	0.690
Proximal Front-Door	0.945	0.941	0.945	0.941	0.595	0.595	0.595	0.597

Table 2: **Varied $A \rightarrow Y$ Effect** experiments. Width and Coverage of 95% bootstrap confidence interval as we vary the $A \rightarrow Y$ direct effect. Z and M are Gaussian, we compute intervals with 64 bootstrap resamplings, and each dataset contains 4000 samples. The $A \rightarrow Y$ direct effect is parameterized by a single coefficient in our linear DGP.

Metric	Gaussian Z, M				Binary Z, M			
	0	0.2	0.4	0.8	0	0.2	0.4	0.8
$Z \rightarrow M \rightarrow W$								
Oracle Backdoor	0.008	0.008	0.008	0.007	0.041	0.040	0.041	0.048
Naive Front-Door	1.041	1.041	1.040	1.040	0.978	0.978	0.979	0.982
Simple Proximal	0.012	0.319	0.985	1.404	0.065	0.081	0.104	0.208
Proximal Front-Door	0.008	0.009	0.010	0.007	0.044	0.046	0.046	0.054

Table 3: **Varied $Z \rightarrow M \rightarrow W$ Effect** experiments. Percent absolute bias as we vary the path-specific effect of $Z \rightarrow M \rightarrow W$ for either Gaussian or binary Z and M . Each dataset contains 4000 samples. The effect is parameterized by the $Z \rightarrow M$ and $M \rightarrow W$ coefficients, which we set to the same value.

that when $\beta_{AY} = 0$, the naive front-door estimator’s assumptions are met and it achieves coverage that is comparable with both the oracle method and the proximal front-door, but does so with an interval that is narrower than either. However, as β_{AY} increases, the naive front-door estimator coverage quickly drops to 0 while the proximal front-door method maintains the same coverage and similar interval widths. The simple proximal method produces wide intervals with zero coverage for all values of β_{AY} , as its assumptions do not depend on this direct effect.

Varied $Z \rightarrow M \rightarrow W$ Effect When $Z \rightarrow M \rightarrow W$ path in Figure 2(d) is 0, marginalizing out M gives us the DAG in Figure 1 (c). This explains the low error of the simple proximal estimator in the 0 columns of Table 3. However, as soon as the coefficients controlling that path-specific effect increase, assumptions (1) and (2) – necessary for the simple proximal estimator’s derivation in Equation (8) – are violated and the estimator’s bias increases.

Varied $Z \leftarrow U \rightarrow W$ Effects For our final set of simulation studies, we consider the completeness assumptions that require Z and W to be effective proxies for U . To explore this assumption, we vary the coefficients that control the direct effect of U on both Z and W . When these coefficients are zeroed out, it violates the completeness assumptions given

Metric	Bootstrap Interval Coverage				Bootstrap Interval Width			
	0	0.2	0.4	0.8	0	0.2	0.4	0.8
$Z \leftarrow U \rightarrow W$								
Oracle Backdoor	0.934	0.938	0.898	0.938	0.317	0.315	0.315	0.312
Naive Front-Door	0.000	0.000	0.000	0.000	0.266	0.267	0.269	0.271
Simple Proximal	0.242	0.070	0.043	0.000	0.492	0.538	1.467	1.411
Proximal Front-Door	0.465	0.902	0.938	0.926	0.860	2.529	1.688	0.641

Table 4: **Varied $Z \leftarrow U \rightarrow W$ Effect** experiments. Width and Coverage of 95% bootstrap confidence interval as we vary the $Z \leftarrow U \rightarrow W$ effects. Z and M are Gaussian, we compute intervals with 64 bootstrap resamplings, and each dataset contains 4000 samples. These effects are parameterized by the $U \rightarrow W$ and $U \rightarrow Z$ coefficients, which we set to the same value.

by (6) and (22). As these assumptions are essential to learning the bridge functions in (5) and (21), we should expect both proximal methods to perform poorly in this setting.

Table 4 shows the width and coverage of a bootstrap confidence interval for each of the four methods as we vary the direct effect of U on its proxies. We see that when these coefficients are 0, both proximal methods have low coverage. As the coefficient values increase, the proximal front-door quickly increases in coverage to approach that of the oracle. We do not see a similar improvement in the simple proximal method because we have not removed the $Z \rightarrow M \rightarrow W$ path-specific effect.

The interval widths in Table 4 tell an interesting story. When the coefficients controlling $Z \leftarrow U \rightarrow W$ are 0, both proximal methods have relatively narrow intervals. As the coefficients increase from 0 to 0.8, simple proximal’s width increases from 0.5 to 1.4. However, proximal front-door’s width jumps from 0.9 to 2.5 as the coefficients increase from 0 to 0.2, but then its width *decreases* to 1.7 and then 0.6 as the coefficients continue to increase. This suggests that when the coefficients controlling $Z \leftarrow U \rightarrow W$ are 0, the bridge function in Equation (21) is essentially undefined, so the GMM function returns an arbitrary result that does not properly encode its uncertainty. As the coefficients increase slightly, the method becomes unbiased but has high variance, resulting in wide intervals that nonetheless provide good coverage. As the coefficients continue to increase, the method becomes less variable and coverage improves while the interval narrows.

8.5 Discussion and Limitations

We have considered a multitude of simulation studies that are designed to comprehensively evaluate the proximal front-door estimator. We show how it generalizes both the front-door estimator and the simple proximal estimator by handling assumption violations of either method. In our results in Tables 1 and 3, the proximal front-door estimator has bias comparable to that of the oracle method. In Table 2 the proximal front-door interval width is within a factor of 2 of the oracle while providing the same coverage. These results suggest it can be an empirically effective approach for recovering from unobserved confounding, as long as the completeness assumption explored in Table 4 is met.

Despite these findings, our simulation studies are limited by the simplifying assumptions we have made. Unlike the derivation in Equation (24), we consider only univariate U , C , Z , M , and W . We also only consider linear effects without interaction terms in our DGP. Future work should consider these extensions, but they are not necessary to highlight the

empirical behavior of the proximal front-door estimator. We release our code to enable future work, including sampling details necessary to precisely replicate our tables, as an Appendix.

9. Conclusions

We have introduced the proximal ID algorithm, a synthesis of proximal causal inference, and non-parametric identification theory based on graphical causal models.

On the one hand, the proximal ID algorithm is able to obtain identification in cases where the classical ID algorithm fails by exploiting additional assumptions involving proxy variables. On the other hand, the proximal ID algorithm greatly extends the applicability of proximal causal inference methods by taking advantage of graphical identification theory.

We described a number of important special cases of the algorithm, the proximal front-door criterion (Pearl, 1995), and proximal extensions of the g-computation algorithm (Robins, 1986). Since estimation methods for the functionals arising in the latter case have already been considered in the literature, we illustrate, by means of simulation studies, estimation for the proximal front-door functional.

The validity of the output of the proximal ID algorithm relies on a correctly specified graphical causal model, as well as the existence of proxy variables and completeness conditions that must hold within certain subproblems encountered by the algorithm.

References

- Joshua D. Angrist and Alan B. Krueger. Instrumental variables and the search for identification: From supply and demand to natural experiments. *Journal of Economic Perspectives*, 15(4):69–85, 2001.
- A. Philip Dawid. Conditional independence in statistical theory. *Journal of the Royal Statistical Society*, 41:1–31, 1979.
- Amanda Gentzel, Dan Garant, and David Jensen. The case for evaluating causal models using interventional measures and empirical data. In *Advances in Neural Information Processing Systems*, pages 11722–11732, 2019.
- Miguel A Hernán and James M Robins. Causal inference, 2010.
- Yimin Huang and Marco Valtorta. Pearl’s calculus of interventions is complete. In *Twenty Second Conference On Uncertainty in Artificial Intelligence*, 2006.
- Manabu Kuroki and Judea Pearl. Measurement bias and effect restoration in causal inference. *Biometrika*, 101:423–437, 2014.
- Steffan L. Lauritzen. *Graphical Models*. Oxford, U.K.: Clarendon, 1996.
- Wang Miao, Zhi Geng, and Eric J Tchetgen Tchetgen. Identifying causal effects with proxy variables of an unmeasured confounder. *Biometrika*, 105(4):987–993, 2018a.
- Wang Miao, Xu Shi, and Eric Tchetgen Tchetgen. A confounding bridge approach for double negative control inference on causal effects. *arXiv preprint arXiv:1808.04945*, 2018b.
- Judea Pearl. Causal diagrams for empirical research. *Biometrika*, 82(4):669–709, 1995. URL citeseer.ist.psu.edu/55450.html.

- Judea Pearl. *Causality: Models, Reasoning, and Inference*. Cambridge University Press, 2 edition, 2009. ISBN 978-0521895606.
- Thomas S. Richardson and Jamie M. Robins. Single world intervention graphs (SWIGs): A unification of the counterfactual and graphical approaches to causality. *preprint: <http://www.csss.washington.edu/Papers/wp128.pdf>*, 2013.
- Thomas S. Richardson, Robin J. Evans, James M. Robins, and Ilya Shpitser. Nested Markov properties for acyclic directed mixed graphs, 2017. Working paper.
- James M. Robins. A new approach to causal inference in mortality studies with sustained exposure periods – application to control of the healthy worker survivor effect. *Mathematical Modeling*, 7: 1393–1512, 1986.
- James M. Robins, Andrea Rotnitzky, and Lue P. Zhao. Estimation of regression coefficients when some regressors are not always observed. *Journal of the American Statistical Association*, 89: 846–866, 1994.
- Xu Shi, Wang Miao, Jennifer C Nelson, and Eric J Tchetgen Tchetgen. Multiply robust causal inference with double-negative control adjustment for categorical unmeasured confounding. *Journal of the Royal Statistical Society: Series B (Statistical Methodology)*, 82(2):521–540, 2020.
- Ilya Shpitser and Judea Pearl. Identification of joint interventional distributions in recursive semi-Markovian causal models. In *Proceedings of the Twenty-First National Conference on Artificial Intelligence (AAAI-06)*. AAAI Press, Palo Alto, 2006a.
- Ilya Shpitser and Judea Pearl. Identification of conditional interventional distributions. In *Proceedings of the Twenty Second Conference on Uncertainty in Artificial Intelligence (UAI-06)*, pages 437–444. AUAI Press, Corvallis, Oregon, 2006b.
- Ilya Shpitser and Eli Sherman. Identification of personalized effects associated with causal pathways. In *Proceedings of the 34th Annual Conference on Uncertainty in Artificial Intelligence (UAI-18)*, 2018.
- Eric J Tchetgen Tchetgen, Andrew Ying, Yifan Cui, Xu Shi, and Wang Miao. An introduction to proximal causal learning. *arXiv preprint [arXiv:2009.10982](https://arxiv.org/abs/2009.10982)*, 2020.
- Jin Tian. Identifying dynamic sequential plans. In *Proceedings of the Twenty-Fourth Conference Annual Conference on Uncertainty in Artificial Intelligence (UAI-08)*, pages 554–561, Corvallis, Oregon, 2008. AUAI Press.
- Jin Tian and Judea Pearl. On the testable implications of causal models with hidden variables. In *Proceedings of the Eighteenth Conference on Uncertainty in Artificial Intelligence (UAI-02)*, volume 18, pages 519–527. AUAI Press, Corvallis, Oregon, 2002.
- Anastasios Tsiatis. *Semiparametric Theory and Missing Data*. Springer-Verlag New York, 1st edition edition, 2006.
- Mark J Van der Laan, MJ Laan, and James M Robins. *Unified methods for censored longitudinal data and causality*. Springer Science & Business Media, 2003.
- Thomas S. Verma and Judea Pearl. Equivalence and synthesis of causal models. Technical Report R-150, Department of Computer Science, University of California, Los Angeles, 1990.
- Philip G. Wright. *The Tariff on Animal and Vegetable Oils*. The Macmillan Company, 1928.